JOURNAL OF PETROLOGY | VOLUME 54 | NUMBER 12 | PAGES 2487–2520 | 2013 | doi:10.1093/petrology/egt054

The Geochemistry and Sm–Nd Isotopic Systematics of Precambrian Mafic Dykes and Sills in the Southern Prince Charles Mountains, East Antarctica

E. V. MIKHALSKY[1]*, S. D. BOGER[2] AND F. HENJES-KUNST[3]

[1]VNIIOKEANGEOLOGIA, ANGLIISKII PR., 1, ST PETERSBURG 190121, RUSSIA

[2]SCHOOL OF EARTH SCIENCES, THE UNIVERSITY OF MELBOURNE, VIC. 3010, AUSTRALIA

[3]BUNDESANSTALT FÜR GEOWISSENSCHAFTEN UND ROHSTOFFE, STILLEWEG, 2, HANNOVER 30655, GERMANY

RECEIVED JANUARY 21, 2013; ACCEPTED AUGUST 30, 2013
ADVANCE ACCESS PUBLICATION OCTOBER 11, 2013

Mafic dykes are a characteristic geological feature of the Ruker Complex in the southern Prince Charles Mountains. We present new geological, geochemical, and Sm–Nd isotopic data for these rocks, which place constraints on their genesis, mantle sources, and relative timing, as well as providing a substantial basis for a comparison between these intrusions and similar rocks from other Archaean terranes of East Antarctica. The oldest of the intrusions form dykes composed of distinctive rocks rich in Mg, Cr, and Ni. These rocks were probably derived via varying degrees of partial melting of a metasomatically enriched and radiogenic mantle source at relatively shallow mantle levels. Younger and volumetrically more significant dykes are composed of subalkaline tholeiite. These tholeiitic dykes strike ENE, NW or NNE and can be divided into two geochemically distinct subgroups: a low-LILE (large ion lithophile element) group (mostly the NNE-trending dykes) and a high-LILE group (NW-trending and partly other directions). The low-LILE group rocks originated from an enriched mid-ocean ridge basalt-like source and are characterized by relatively young Sm–Nd T_{DM} model ages between 1·9 and 2·4 Ma. The high-LILE group rocks have higher LILE/HFSE (high field strength element) ratios, which imply derivation from an enriched subcontinental mantle source. These rocks have generally older T_{DM} model ages between 2·3 and 3·8 Ga and display geochemical similarities to mafic metavolcanic rocks found within the Palaeoproterozoic Ruker Group, a cover sequence to the Archaean Ruker Complex. As was observed by earlier researchers, the subalkaline tholeiitic dykes in the Ruker Complex have many compositional features in common with mafic dykes from the Napier Complex of Enderby Land and from the Vestfold Hills. However, our data do not provide convincing evidence for a direct correlation with these dyke suites. The youngest phase of mafic intrusions comprises distinctive high-Ti–P rocks that occur as sills within the Neoproterozoic Sodruzhestvo Group, another cover sequence to the Ruker Complex. The high-Ti–P rocks do not correlate with any of the dyke suites observed within the Ruker Complex, nor from elsewhere in East Antarctica. They are interpreted to represent manifestations of plume-related magmatism associated with extension, subsidence, and accumulation of the Sodruzhestvo Group.

KEY WORDS: *Antarctica; geochemistry; mafic dykes; Proterozoic; Sm–Nd systematics*

INTRODUCTION

Mafic dykes are common cross-cutting features observed in the Archaean complexes of the Enderby Land to Princess Elizabeth Land sector of East Antarctica (Fig. 1). The Archaean complexes include the Napier Complex of Enderby Land (Sheraton & Black, 1981; Black & James, 1983) together with its reworked margin in Kemp Land (Kelly *et al.*, 2004; Halpin *et al.*, 2005), the Vestfold Hills Complex of Princess Elizabeth Land (Collerson & Sheraton, 1986) and the Archaean components of the southern Prince

*Corresponding author. E-mail: emikhalsky@mail.ru

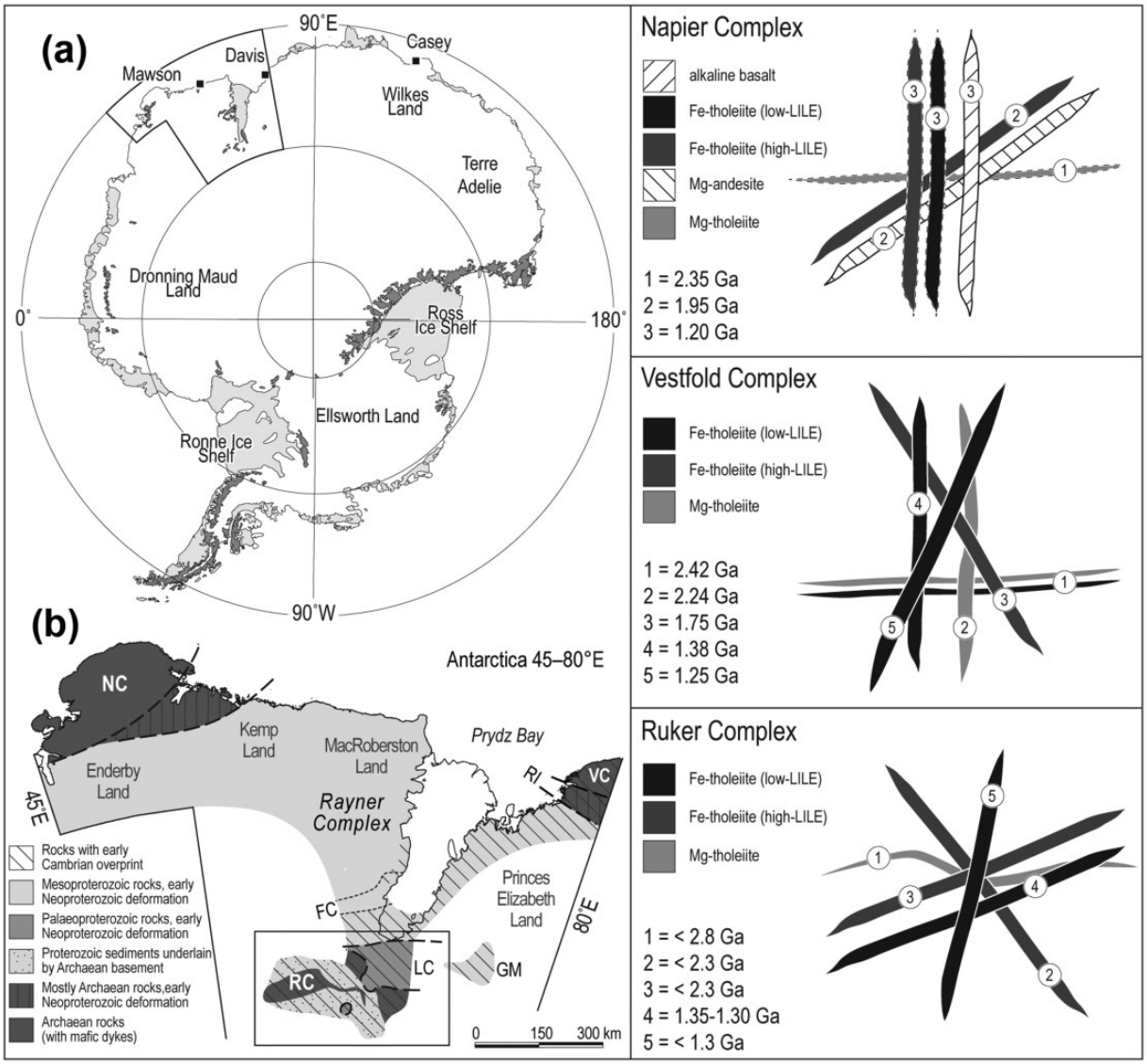

Fig. 1. Location maps of the study area. (a) Antarctica with the location of the study area highlighted with a polygon. Areas in dark grey are outcrop, areas in light grey are ice shelves. (b) East Antarctica between 45 and 80°E illustrating the regional geology of the Amery Ice Shelf–Prydz Bay region (after Corvino *et al.*, 2011). Location abbreviations: FC, Fisher Complex; GM, Grove Mountains; LC, Lambert Complex; NC, Napier Complex; RC, Ruker Complex; RI, Rauer Islands; VC, Vestfold Hills Complex. Right-hand schematic illustrations show the composition, orientation, relative emplacement order and available age data for mafic dykes in the Napier Complex of Enderby Land (Sheraton & Black, 1981; Suzuki *et al.*, 2008), in the Vestfold Complex (Collerson & Sheraton, 1986; Hoek & Seitz, 1995; Mikhalsky, 1995) and in the Ruker Complex (Mikhalsky *et al.*, 2007; this study).

Charles Mountains (sPCM) (Kamenev *et al.*, 1993; Boger *et al.*, 2006; Mikhalsky *et al.*, 2006*a*; Phillips *et al.*, 2006). Within the southern Prince Charles Mountains mafic dykes are found in the Menzies Group and Mawson Suite of the Ruker Complex (Boger *et al.*, 2006; Phillips *et al.*, 2009) and within the middle Archaean Manning Orthogneiss of the adjacent Lambert Complex (Boger *et al.*, 2008). Dykes are, however, mainly absent from the Palaeoproterozoic rocks of the Lambert Complex, and the Mesoproterozoic Rayner Complex (Mikhalsky *et al.*, 2006*b*) that separate the inland southern Prince Charles Mountains from the Napier and Vestfold complexes on the coast (Fig. 1). This observation has allowed the presence or absence of dykes to be used as temporal stratigraphic markers (Tingey, 1982, 1991).

Little is known about the mafic dykes observed in the sPCM. They are variably deformed and locally metamorphosed (Mikhalsky *et al.*, 2001) and, based on limited geochemical data, show some similarities to the dykes observed in the Napier Complex and the Vestfold Hills (Sheraton *et al.*, 1987; Srivastava *et al.*, 2000). On the basis of these similarities, the sPCM dykes were assumed to be

of similar Mesoproterozoic age (Sheraton & Black, 1981; Collerson & Sheraton, 1986; Sheraton *et al.*, 1987; Srivastava *et al.*, 2000). At present, however, the only geochronological data reported from the sPCM are a single Pb-evaporation $^{207}Pb/^{206}Pb$ zircon age of *c.* 2370 Ma (Th/U = 0·336) from a high-Mg dyke exposed in the southern Mawson Escarpment (Mikhalsky *et al.*, 1992) and a U–Pb zircon age of *c.* 1350–1300 Ma from a single zircon recovered from a tholeiitic dyke in McCue Bluff (Mikhalsky *et al.*, 2007). Until now it remains unknown how many dyke suites are actually present in the sPCM, nor are the chemistry, age, and timing relationships between these rocks well understood—certainly not sufficiently well to allow for reliable comparisons to be made between the sPCM mafic dykes and those exposed in the Napier and the Vestfold Hills complexes (Fig. 1).

Here we present new geological, geochemical and Sm–Nd whole-rock isotopic data for mafic intrusions from a wide area of the sPCM (Fig. 2). The rocks sampled represent undeformed to slightly deformed dykes with clear, sharp cutting relationships to their country rocks (Fig. 3a–c). Samples were collected from Rimmington and McCue Bluffs, prominent outcrops exposed along the southern Mawson Escarpment, as well as from Mounts Stinear and Rymill, the Cumpston Massif, and some other localities (Fig. 2). The data presented provide petrogenetic constraints on the origin of the observed mafic intrusions in the sPCM and allow a more detailed comparison between these rocks and the mafic dykes from other East Antarctic regions. These data were mostly collected by the authors during the Prince Charles Mountains Expedition of Germany and Australia (PCMEGA) in 2002–2003, and by S. D. Boger during his work in the same area in 1997–1998. Geochemical data (X-ray fluorescence) acquired by the early Australian expeditions to the same area were kindly provided by Dr J. W. Sheraton. Some geological observations and chemical analyses obtained by Russian scientists from expeditions dating back to the late 1980s are also included.

MAFIC DYKE SUITES IN OTHER ANTARCTIC ARCHAEAN TERRANES

In the Napier Complex, at least three dyke suites of Proterozoic age have been recognized. The oldest suite consists of high-Mg dykes, which vary in composition from hypersthene-rich olivine-normative tholeiite (norite) to hypersthene-bearing quartz tholeiite. These rocks have yielded a Rb–Sr whole-rock isochron age of 2350 ± 48 Ma (Sheraton & Black, 1981). This suite was followed by the emplacement of a NE-trending suite of dykes dated at 2150–1900 Ma on the basis of Rb–Sr and Sm–Nd isochrons (Suzuki *et al.*, 2008). Dykes of this age can be subdivided

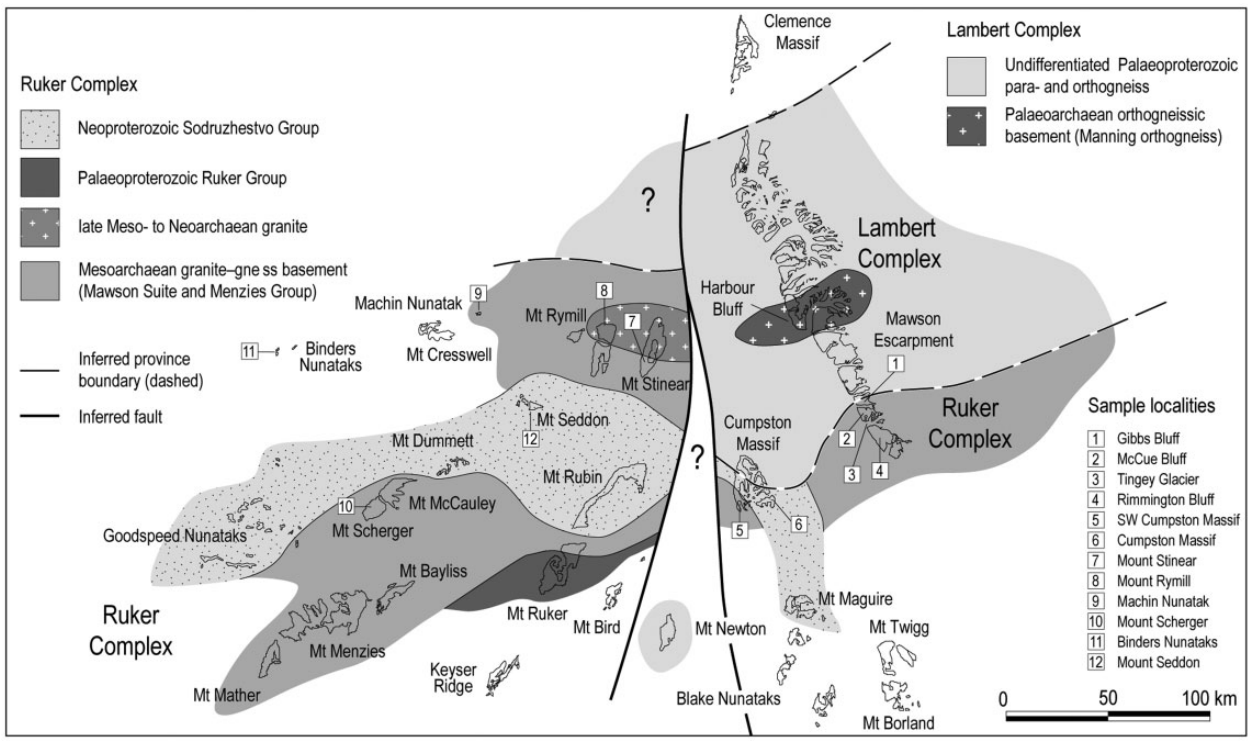

Fig. 2. Geology of the southern Prince Charles Mountains (modified from Mikhalsky *et al.*, 2001; Phillips *et al.*, 2009; Corvino *et al.*, 2011).

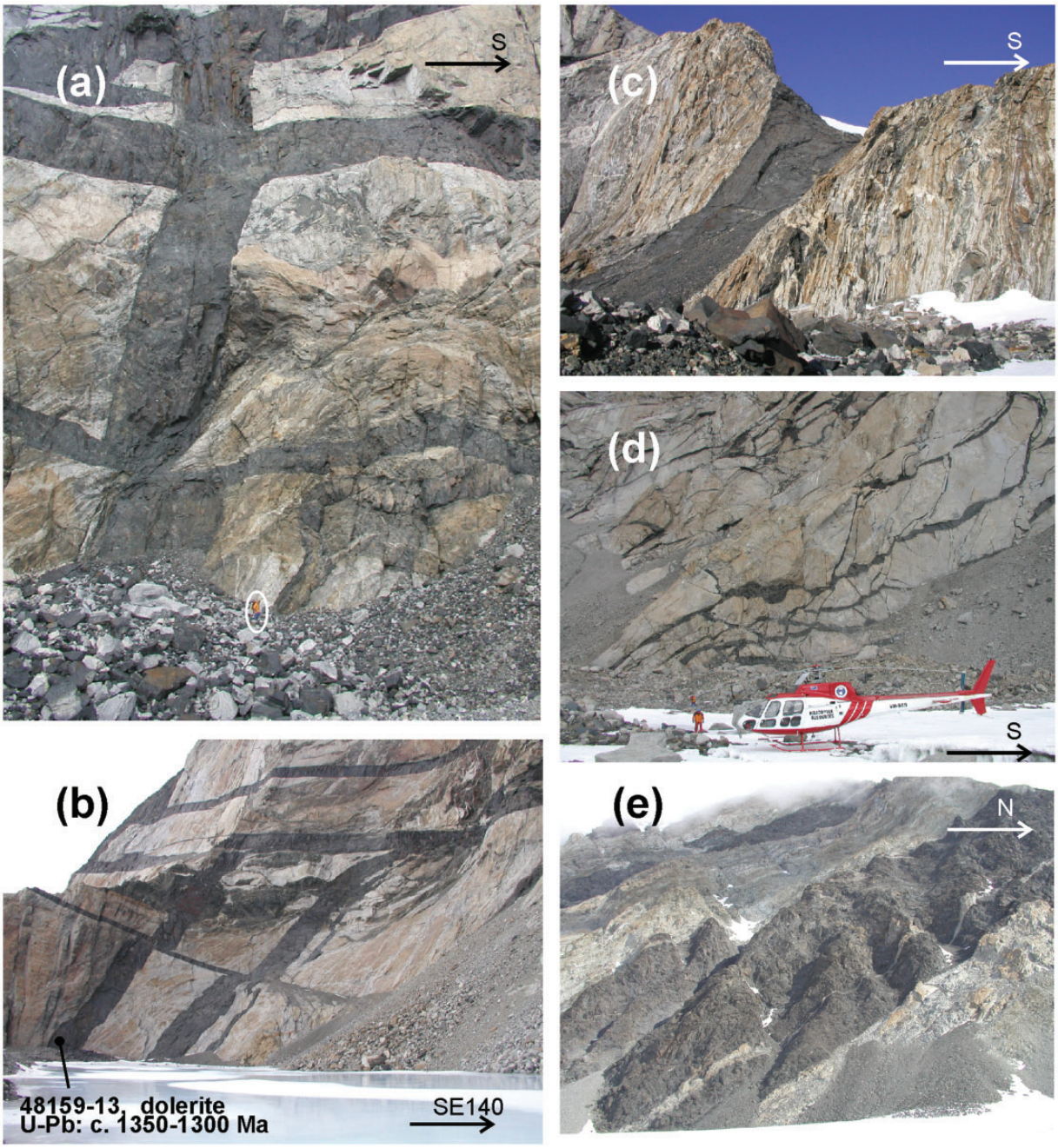

Fig. 3. Mafic dyke (a–d) and sill (e) occurrences in the southern Prince Charles Mountains. (a) A vertical ENE-trending dolerite dyke, apparently transected by unsampled (NNE-trending) dykes and shear zones (presumably of latest Neoproterozoic to Cambrian age; Boger *et al.*, 2006; Phillips *et al.*, 2009) gently dipping to the ESE, and an older high-Mg curved dyke (in the right-hand corner), central McCue Bluff (note person outlined with white oval for scale). (b) Similar dykes suites to those in (a), northern McCue Bluff (note apparently post-1350 Ma NNE-striking dykes and shear zones). (c) A thick vertical NW-trending metamorphosed dyke, north Tingey Glacier. (d) A network of sheared dykes, the southwestern part of Cumpston Massif. (e) A sill within Neoproterozoic metasediments, Cumpston Massif; outcrop height is about 250–300 m.

into two compositional groups: tholeiite and high-Mg andesite. Both groups exhibit large ion lithophile element (LILE) and light rare earth element (LREE) enrichment and negative Nb and Ti anomalies in primitive mantle normalized trace element patterns (Suzuki *et al.*, 2008). Suzuki *et al.* observed a correlation of increasing trace element concentrations with increasing FeO*/MgO and attributed the geochemical features of both groups to

either subduction-related arc magmatism or continental flood basalt volcanism. The youngest dykes belong to the 1190 ± 200 Ma Amundsen suite (Rb–Sr whole-rock isochron; Sheraton & Black, 1981). These rocks are of quartz tholeiitic composition and are divided into two compositional types on the basis of differing trace element geochemistry. The Group I tholeiites have higher contents of some incompatible elements including LILE (K, Rb, Sr), LREE and high field strength elements (HFSE, P, Zr, Nb) compared with Group II dykes. Group I dykes also have slightly lower average magnesium numbers [mg number = 100MgO/(MgO + FeO^{tot}), mol %], 43 vs 46, when compared with the Group II rocks (Sheraton & Black, 1981). Group II dykes are characterized by marked negative Nb anomalies, a feature not observed for the Group I rocks. Sheraton & Black (1981) pointed out that the compositions of Group I rocks cannot be attributed to more extensive crystal fractionation. Of similar age (1161 ± 238 Ma, a whole-rock Rb–Sr isochron) are alkaline basalts characterized by relatively high concentrations of P, Ti, Ba, Sr, Nb and LREE (Suzuki *et al.*, 2008). These rocks are chemically distinct from the Amundsen suite as defined by Sheraton & Black (1981) although at present they are not temporally differentiable.

The Vestfold Hills preserve evidence for five phases of high-Mg and/or tholeiitic mafic magmatism (Kuehner, 1987; Hoek & Seitz, 1995). The oldest event resulted in the emplacement of east-trending high-Mg (gabbronorite–dolerite) and high-Fe tholeiitic (dolerite) dykes that are dated to 2424 ± 72 Ma (Rb–Sr whole-rock isochron; Collerson & Sheraton, 1986). The second phase of magmatism led to the emplacement of a norite ring complex and a coeval but relatively uncommon north-trending suite of high-Mg tholeiitic dykes (Hoek & Seitz, 1995). U–Pb zircon ages of 2241 ± 4 Ma and 2238 ± 7 Ma were obtained from felsic segregations associated with this phase of magmatism (Lanyon *et al.*, 1993). The third phase of mafic magmatism resulted in the emplacement of NW-trending Fe-rich tholeiites (Hoek & Seitz, 1995), which are dated by a whole-rock Rb–Sr isochron at 1791 ± 62 Ma (Collerson & Sheraton, 1986) and zircon sensitive high-resolution ion microprobe (SHRIMP) studies at 1754 ± 16 Ma (Lanyon *et al.*, 1993). During the fourth phase north-trending Fe-rich tholeiitic dykes were emplaced. These were dated at 1380 ± 7 Ma (Lanyon *et al.*, 1993). The final magmatic episode led to the emplacement of the densest of the observed dyke swarms. These rocks are defined by NNE-trending Fe-rich tholeiites that were emplaced around 1245 Ma based on two zircon ages of 1248 ± 4 Ma (Black *et al.*, 1991) and 1241 ± 5 Ma (Lanyon *et al.*, 1993).

The high-Mg tholeiites from suites one (*c.* 2425 Ma) and two (*c.* 2240 Ma) are characterized by relatively high SiO_2 and MgO, but low TiO_2. They are enriched in some LILE (Ba, Rb, and K) and LREE and show pronounced negative Nb, P and Ti anomalies (Collerson & Sheraton, 1986; Kuehner, 1989; Hoek & Seitz, 1995). Rocks of the first suite do not show a negative Sr anomaly, whereas the norites and north-trending dykes of the second suite do (Hoek & Seitz, 1995). The first suite also comprises the Fe-rich tholeiites, which, compared with the high-Mg tholeiites, are notably less siliceous and contain lower average abundances of LILE.

The Fe-rich tholeiites of the third suite (*c.* 1750 Ma) were distinguished by Collerson & Sheraton (1986) as Group I tholeiites and exhibit a wide range in incompatible trace element abundances. Normalized trace element patterns are, however, similar and are characterized by marked negative Nb and Sr anomalies, as described by Collerson & Sheraton (1986) and Hoek & Seitz (1995). Those researchers suggested that these rocks were derived from an LILE-enriched mantle source. In a study preceding the dating of these dykes, Collerson & Sheraton (1986) recognized geochemically distinct Group II and Group III tholeiites within the younger (*c.* 1380 Ma and *c.* 1245 Ma) dyke suites. Group II tholeiites contain lower trace element concentrations (P, Sr, Nb, La, Ce, etc.) than Group I at a given mg number (Collerson & Sheraton, 1986). Group III was characterized by only a few analyses, and these rocks were enriched in LILE. Subsequent studies have shown that the rocks of the fourth (*c.* 1380 Ma, north-trending) and the fifth suites (*c.* 1250 Ma, NNE-trending) show similar overall trace element patterns, but the former tends to have higher normalized trace element abundances (Hoek & Seitz, 1995; Mikhalsky, 1995). Similar to the two older Fe-rich tholeiite suites, these rocks show a distinct negative Nb anomaly. Unfortunately, the full datasets obtained in these earlier studies were not published, to the best of the authors' knowledge.

GEOLOGICAL SETTING

Cropping out between 60 and 70°E and south of latitude 73°S, the sPCM represent the southernmost exposures of rock found within the Prince Charles Mountains–Prydz Bay region. The range was first visited by Australian expeditions in 1954, with subsequent visits in the late 1950s providing the first geological descriptions of the area (Stinear, 1956; Crohn, 1959; McLeod, 1959). These studies were built upon by further reconnaissance studies in the 1960s (Ruker, 1963; Trail, 1963*a*, 1963*b*, 1964; McLeod, 1964) and then more focused mapping in the 1970s (Tingey & England, 1973; England & Langworthy, 1975; Tingey *et al.*, 1981). Soviet geologists were also active in the sPCM between 1971 and 1974. The results of these studies were presented in a number of early publications from the 1970s (Soloviev, 1972; Grikurov & Soloviev, 1974) but have been more fully described in the *Antarctic Geoscience* compilation published in 1982 (Fedorov *et al.*, 1982; Kamenev, 1982; Lopatin & Semenov, 1982; Ravich, 1982; Ravich &

Fedorov, 1982) and in a book by Ravich and others published a few years later (Ravich *et al.*, 1985).

On the basis of these studies and the results of more recent work cited below, the sPCM can be broken into two geologically distinct tectonic complexes: the Ruker and Lambert complexes (Kamenev *et al.*, 1993; Mikhalsky *et al.*, 2006*a*; Fig. 2). The Ruker Complex, the focus of this study, comprises an Archaean granite–gneiss basement defined by the Mawson Suite and Menzies Group, together with two or more sequences of sedimentary and volcanic cover rocks (Ravich *et al.*, 1985; Kamenev *et al.*, 1993; Mikhalsky *et al.*, 2001; Phillips *et al.*, 2009). The Mawson Suite consists of well-dated felsic intrusions that were emplaced at 3390–3380 Ma and 3180–3160 Ma (Boger *et al.*, 2006, 2008; Mikhalsky *et al.*, 2006*a*, 2010). The Menzies Group consists of thick horizons of quartzite intercalated with rocks of volcanic, terrigenous, and chemical origin. Detrital zircons from the Menzies Group suggest a maximum depositional age of *c.* 3150 Ma (Phillips *et al.*, 2006).

Deformation post-dating both the emplacement of the Mawson Suite and deposition of the Menzies Group resulted in both layer-parallel and upright generations of overprinting folds (Boger *et al.*, 2006). Metamorphic grade varies from lower to upper amphibolite facies (Grew, 1982; Kamenev *et al.*, 1993; Mikhalsky *et al.*, 2001; Phillips *et al.*, 2005). Metamorphism is dated at 2780 Ma from the southern Mawson Escarpment (Boger *et al.*, 2006), whereas syntectonic granitic intrusions (*c.* 2815 Ma) are known from Mts Stinear, Bayliss and Rymill (Mikhalsky *et al.*, 2010).

The Ruker and Sodruzhestvo Groups, which both postdate 2820–2780 Ma orogenesis observed in the granite–gneiss basement, define the remaining strata of the Ruker Complex (Mikhalsky *et al.*, 2001). At its type locality at Mt Ruker, the Ruker Group is defined by a well-layered sequence of mainly basic volcanic rocks intercalated with ironstones as well as terrigenous and calcareous sedimentary rocks (Grew, 1982; Mikhalsky *et al.*, 2001; Phillips *et al.*, 2005). Minor intrusions of metamorphosed gabbro–dolerite, mostly as sills but also locally as dykes, are found within the lower section of the Ruker Group (Mikhalsky *et al.*, 2001; Phillips *et al.*, 2005). Detrital zircons from the upper Ruker Group give ages between 3300 and 2450 Ma and limit the deposition of these strata to the early Palaeoproterozoic (Phillips *et al.*, 2006).

The Sodruzhestvo Group crops out at Mounts Rubin, Dummett, Seddon and Maguire, as well as at Cumpston Massif and Goodspeed Nunataks (Mikhalsky *et al.*, 2001; Phillips *et al.*, 2005, 2006). This group consists of quartzite, well-layered semi-pelitic schist and comglomerate (Mikhalsky *et al.*, 2001, and references therein). These rocks are further characterized by their lower metamorphic grade—they do not exceed the greenschist facies—and the general absence of mafic dykes in most localities. Mafic sills are, however, present in the Sodruzhestvo Group at Cumpston Massif (Phillips *et al.*, 2005) and Mt Seddon (Ravich *et al.*, 1985). The age of these rocks is constrained to the Neoproterozoic (<970 Ma) based on both microfossil and detrital zircon data (Iltchenko, 1972; Phillips *et al.*, 2006) and the group may be up to 11 km thick based on geophysical modeling (McLean *et al.*, 2008). Deformation in the Sodruzhestvo Group resulted in the formation of a single generation of upright to inclined NW-trending folds (Phillips *et al.* 2005) that are constrained to have formed between 520 and 495 Ma (Phillips *et al.*, 2007).

The Lambert Complex, exposed to the north of the Ruker Complex and possibly also in the Mt Newton area (Mikhalsky *et al.*, 2008) (Fig. 2), consists of high-grade para- and orthogneisses. Biotite and garnet–biotite ± hornblende gneiss, granite–gneiss, plagiogneiss and mafic to ultramafic granulite or amphibolite are the most common rock types. Ages of *c.* 3520, 2450 and 2120 Ma were obtained for orthogneisses, and a wide time frame (2500–1000 Ma) is suggested for the deposition of the intercalated paragneisses (Boger & Wilson, 2005; Corvino & Henjes-Kunst, 2007; Boger *et al.*, 2008; Corvino *et al.*, 2008). With the exception of the Manning Orthogneiss exposed at Harbour Bluff, the Lambert Complex does not contain mafic dykes. This unit dates to the middle Archaean (*c.* 3520 Ma) and may represent either basement to the predominantly Palaeoproterozoic crust that defines the remainder of the Lambert Complex, or a tectonically intercalated slab of unrelated rock (Boger *et al.*, 2008).

MODE OF DYKE OCCURRENCE

Mafic dykes in the Ruker Complex are limited to the granite–gneiss basement defined by the Mawson Suite and the Menzies Group. Mafic dykes within these rocks commonly form networks of cross-cutting dykes, which, however, can be only rarely observed owing to limited access. The extent of metamorphism and deformation of the dykes varies considerably between localities. In some outcrops the dykes are largely undeformed, as is the case along most of the southern Mawson Escarpment (Fig. 3a–c). Dykes can, however, be sheared, as occurs commonly at Mts Stinear and Rymill and southwestern Cumpston Massif (Fig. 3d), or locally folded; for example, at northern Cumpston Massif. Where undeformed, the dykes can nevertheless be offset by narrow shear zones (Fig. 3a and b), or internally foliated to form mafic schists. In the latter case the dyke boundaries are not usually strongly displaced (Fig. 3d). Deformation features, where developed, are most probably related to early Palaeozoic tectonism, which is widely recorded in the southern Prince Charles Mountains (Boger & Wilson, 2005; Boger *et al.*, 2006; Phillips *et al.*, 2007, 2009; Corvino *et al.*, 2008).

Along the southern Mawson Escarpment mafic dykes are between 2 and 50 m thick and trend in four predominant directions: west (275–285°), NW (300–315°), NNE (0–30°), and ENE (60–75°). The ENE-trending dykes are the most abundant (Fig. 4). Next most abundant is the NW-trending suite, followed by the NNE-trending suite. West-trending dykes are uncommon and are mostly narrow with non-tabular curved shapes, and are chemically distinct from the other dyke suites. Most dykes are steeply dipping, but dips can be variable and in McCue Bluff some dykes have a shallow dip. Rare cross-cutting relationships suggest that the west-trending dykes are the oldest, whereas the NNE-trending suite is the youngest. For all generations, dyke contacts with their country rocks are mostly planar and sharp. Chilled margins are only rarely developed and no phenocrysts were found within these zones or within the dyke interiors.

In addition to the widespread dykes observed within the Ruker Complex, the Sodruzhestvo Group contains mafic sills up to a few tens of meters thick (Fig. 3e) and rare thin steeply dipping dykes (Phillips *et al.*, 2005). The intrusion of these rocks is interpreted to be either synchronous with or post deposition of the Sodruzhestvo Group.

PETROGRAPHY

Given the variable degrees of metamorphic recrystallization, we apply the terms dolerite when the magmatic texture of the rock is only slightly modified, altered dolerite when low-grade alteration is strong, metadolerite or apodolerite when the rock has experienced a metamorphic overprint but the primary magmatic texture can be either easily (metadolerite) or hardly (apodolerite) recognized, amphibolite when the rock has acquired a metamorphic granoblastic texture, and mafic schist when the rock shows both a metamorphic mineral assemblage and a pronounced foliation.

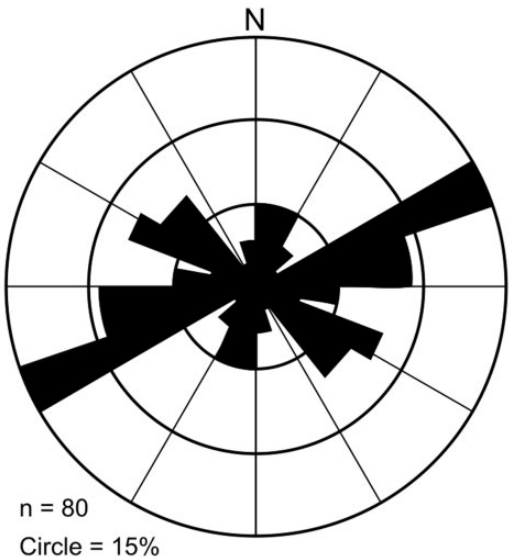

Fig. 4. Rose-diagram for mafic dykes in the southern Mawson Escarpment.

The oldest group of dykes (west-trending) is mostly strongly retrogressed and sheared, and is composed of mafic to ultramafic amphibolite, schist or occasionally noritic metadolerite. The original magmatic textures are only rarely preserved and such rocks have a lamprophyric rather than an ophitic texture (i.e. pyroxene as opposed to plagioclase is euhedral; Fig. 5a). The west-trending dykes are melanocratic (colour index M is mostly 75–80) to ultramafic and relatively coarse-grained (1–3 mm) when compared with the typical dolerites and metadolerites of the other suites. These rocks are composed predominantly of hornblende 70–80% (vol. % here and below when referring to mineral contents), biotite up to 20% and plagioclase <20%. In metadolerites pyroxene is nearly completely replaced by a very fine-grained serpentine aggregate, which in turn is altered to talc, biotite and minor amphibole (Fig. 5b). The secondary products point to primary orthopyroxene, although this mineral was never directly observed. These rocks may thus be termed noritic metadolerite.

The other dykes in the Ruker Complex are less melanocratic (mostly M = 45–70). Fresh dolerites (NNE and ENE dykes) occur at McCue Bluff in the southern Mawson Escarpment. At this locality the dolerites are fine-grained (<0·5 mm) massive rocks with typical doleritic to subophitic textures with a few better-crystallized samples (Fig. 5c). The rocks are composed of *c.* 50–60% isometric or rarely elongated brownish clinopyroxene ($Ca_{29–34}Mg_{47}Fe_{19–24}$) with the remainder of the rock defined by plagioclase laths. Clinopyroxene may be variously altered to green amphibole, biotite and Fe–Ti oxides. Plagioclase is commonly altered to an unidentified clay mineral. These secondary minerals are thought to represent autometamorphic products. Metadolerites (various dyke suites), observed widely at Rimmington Bluff and McCue Bluff, contain 40–70% amphibole, 25–55% andesine to labradoritic plagioclase, up to 10% quartz, up to 4% titanite, and minor biotite, epidote, and Fe–Ti oxides. The Fe–Ti oxides occasionally form skeletal grains of recognizable crystal shape in association with fine-grained amphibole aggregates, or rarely form relatively coarse porphyroblasts. Ilmenite is partly or entirely replaced by titanite.

In the metadolerites, the lowest grade of metamorphic recrystallization resulted in the replacement of clinopyroxene by pale green actinolite. More extensive recrystallization results in the formation of sieve-like aggregates of green hornblende with quartz inclusions in amphibolite or apodolerite (Fig. 5d). Under higher-grade

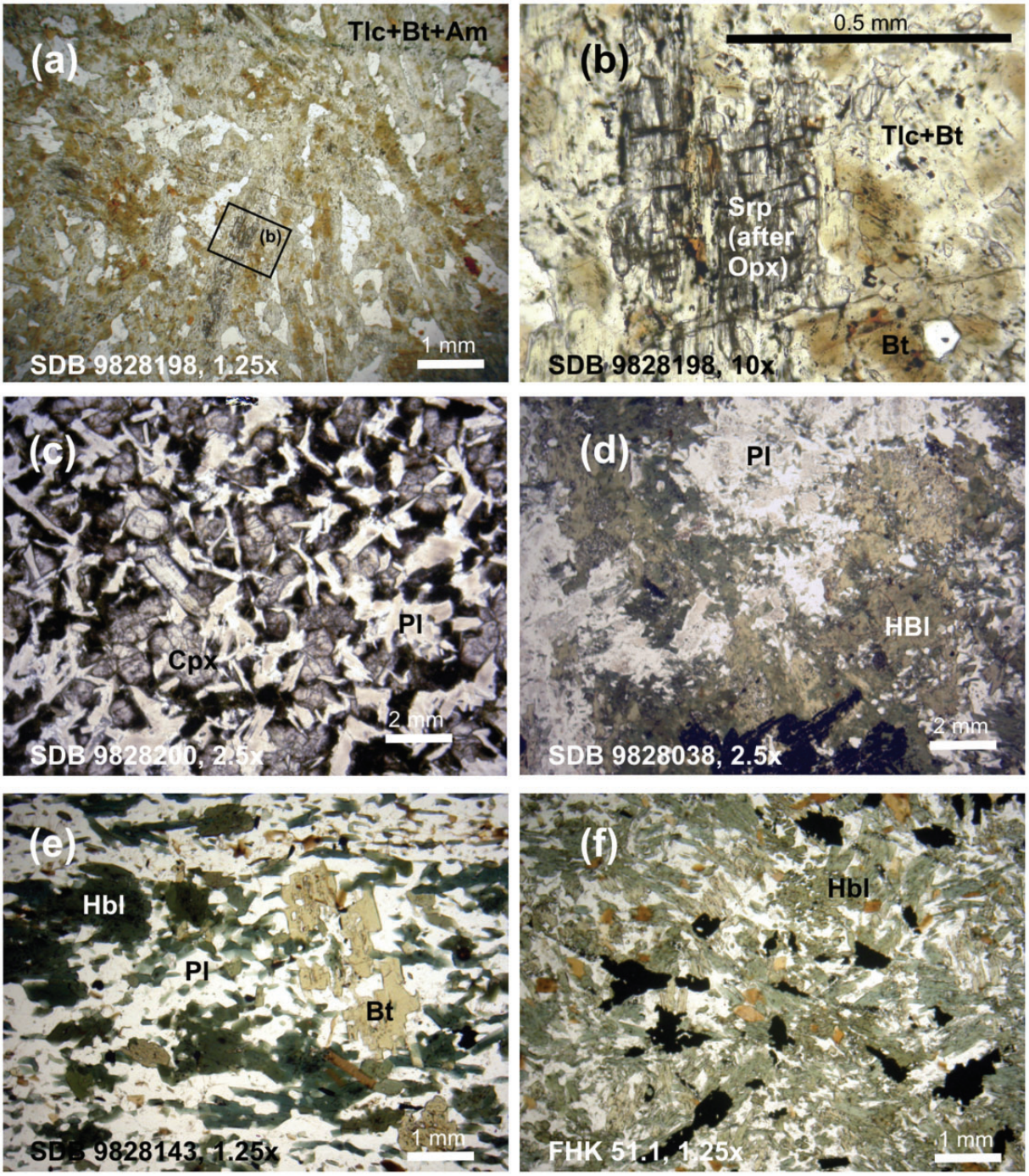

Fig. 5. Photomicrographs of mafic intrusive rocks. (a, b) Noritic metadolerite, McCue Bluff (9828198); (b) is enlargement of box in (a). (c) Dolerite, McCue Bluff (9828200). (d) Apodolerite, McCue Bluff (9828038). (e) Mafic schist, McCue Bluff (9828143). (f) Amphibolite (a sill in the Sodruzhestvo Group, central Cumpston Massif, sPCM51.1). View area in (a), (e) and (f) is 7·5 mm × 5 mm; in (b) 0·9 mm × 0·6 mm; in (c) and (d) 3·75 mm × 2·5 mm.

conditions, granoblastic–polygonal amphibolites with dark green or greenish brown hornblende are formed. In such rocks a strong foliation is commonly observed and these rocks grade into mafic schists (Fig. 5e). The higher modal quartz and lower modal plagioclase observed in the metadolerites and mafic schists when compared with fresh dolerites resulted from breakdown of clinopyroxene and plagioclase to form hornblende and

quartz. Secondary garnet occurs in a few metadolerites. Where present, garnet occurs along contacts between amphibole and plagioclase and forms a mantle surrounding amphibole pseudomorphs after pyroxene.

The mafic sills that crop out within the Sodruzhestvo Group (central Cumpston Massif) are composed of massive, melanocratic (M = 60–80), and characteristically fine-grained (mainly 0·2–0·6 mm) amphibole–plagioclase rocks that show apo-ophitic to nematoblastic textures (Fig. 5f). The mafic minerals consist of 45–60% hornblende (pleochroic between khaki green and bluish green), up to 20% biotite, which forms small randomly oriented flakes, and abundant Fe–Ti oxides that can constitute up to 15% of the rock and form coarser laths up to 2 mm in size. Titanite and apatite are common accessory phases. Some rocks have a coarse-grained nematoblastic texture that shows no preferred orientation of hornblende. Hornblende may be altered to chlorite.

ANALYTICAL METHODS

Major and trace element concentrations were determined by X-ray fluorescence spectrometry (XRF) at the Bundesanstalt für Geowissenschaften und Rohstoffe (BGR, Hannover) and at the University of Melbourne. These new data were augmented with largely unpublished XRF results for 19 samples collected by earlier Australian and Russian expeditions and analysed at BMR (now Geoscience Australia, Canberra). Details of the XRF analytical procedure have been provided by Sheraton & Labonne (1978) and Corvino & Henjes-Kunst (2007). Analytical precision varies from 1–2% for major elements to 5–10% for trace elements. The full dataset is included in the Electronic Appendix (available for downloading at http://www.petrology.oxfordjournals.org) and representative analyses are given in Table 1. REE concentrations for 13 samples (Table 2) were obtained by inductively coupled plasma mass spectrometry (ICP-MS) at VSEGEI (St. Petersburg). Sample powders were dissolved using a lithium metaborate fusion technique, followed by dissolution of the glasses in nitric acid. Analyses were carried out on an ELAN-6100 DRC ICP-MS system and have a precision of better than ±5–10%.

Sm–Nd isotope data were acquired at BGR and the University of Melbourne. In Hannover, 100–125 mg of sample powder were mixed with ^{147}Sm–^{148}Nd spike and dissolved in a PicotraceTM high-pressure sample dissolution system (160°C, HF–HNO_3 for 24–48 h; 6 M HCl for 7–12 h), followed by extraction of Sm and Nd using cation exchange and HDEHP columns. Blanks were negligible. Isotopic analyses were performed on a Finnigan Triton system. Raw Nd isotope ratios were normalized to $^{146}Nd/^{144}Nd = 0{\cdot}7219$, using the exponential law, and data are reported relative to LaJolla Nd = 0·511845. External precision (2SD) is 0·5% ($^{147}Sm/^{144}Nd$) and 0·0025% ($^{143}Nd/^{144}Nd$); the long-term averages for USGS AGV-2 andesite are $0{\cdot}1088 \pm 1$ and $0{\cdot}512775 \pm 12$ [$n = 31$, consistent with thermal ionization mass spectrometry (TIMS) reference values (e.g. Raczek *et al.*, 2003; Weis *et al.*, 2006)]. In Melbourne, 50–100 mg of powder were spiked with ^{149}Sm–^{150}Nd and dissolved in Krogh-type high-pressure vessels (160°C, HF–HNO_3, 48 h; 6 M HCl, 12 h). Sm and Nd were extracted using Eichrom RE and LN resin; blanks were <0·1 ng and negligible. Isotopic analyses were performed on a Nu Plasma MC-ICP-MS (Maas *et al.*, 2005). Nd isotope ratios were normalized to $^{146}Nd/^{145}Nd = 2{\cdot}0719425$ (equivalent to $^{146}Nd/^{144}Nd = 0{\cdot}7219$), using the exponential law as part of an on-line iterative spike-stripping/internal normalization procedure, and data are reported relative to LaJolla Nd = 0·511845. External precision (2SD) is 0·2% ($^{147}Sm/^{144}Nd$) and 0·004% ($^{143}Nd/^{144}Nd$); the long-term averages for USGS BCR-2 andesite are $0{\cdot}1383 \pm 3$ and $0{\cdot}512640 \pm 20$, consistent with TIMS reference values (e.g. Raczek *et al.*, 2000, 2003).

WHOLE-ROCK GEOCHEMICAL DATA

Whole-rock data for the mafic dykes from the Ruker Complex show that they have basic compositions with SiO_2 contents ranging from 45 to 56 wt %. Most rocks are compositionally basalts, with fewer basaltic andesites and picrites (Fig. 6). Magnesium numbers vary from 30 to 70. With the exception of a few samples, the mafic rocks are subalkaline. The rocks that tend to have slightly alkaline compositions are the Neoproterozoic sills observed within the Sodruzhestvo Group. Major elements show a wide range of variation (Figs 7 and 8) suggestive of the occurrence of a number of different rock types. Secondary alteration should also not be discounted, in particular for mobile components, such as Na_2O, K_2O and LILE such as Rb, Sr, Ba and Pb. However, we found no correlation between rock alteration or deformation degree and chemical composition in terms of major and trace elements for the NNE- and ENE-trending dykes for which many analyses were obtained. These rocks vary from fresh dolerite to mafic schist but nevertheless exhibit both limited variations in element concentrations and strongly correlated variations of mg number, Ti, Zr and Th (Fig. 9). Other elements, such as Rb and Sr, do show systematic shifts in metamorphosed samples with Rb depletion and Sr enrichment.

Three major rock groups may be distinguished based on their specific geological position, relative age and chemical composition: (1) high-Mg metabasite; (2) subalkaline tholeiite; (3) high-Ti–P metabasite (Figs 6–8). The high-Mg metabasites comprise the mostly metamorphosed and

Table 1: Major and trace element analyses for representative mafic dykes and sills from the southern Prince Charles Mountains

Sample ID:	33501-8	33501-13	9828198	sPCM D	9828116	sPCM 29.1	9828055	9828038
Locality:	Rimmington Bluff south	Rimmington Bluff south	McCue Bluff	Mt Rymill	Rimmington Bluff	Mt Stinear	Rimmington Bluff	Rimmington Bluff
Suite:[1]		E-W	E-W		E-W		NNE	NNE
Group:	High-Mg	High-Mg	High-Mg	High-Mg	High-Mg	High-Mg	Low-LILE	Low-LILE
Rock:	Amphibolite	Amphibolite	Noritic metadolerite	Apodolerite	Mafic schist	Mafic schist	Apodolerite	Apodolerite
SiO_2	44·89	45·09	50·34	51·84	51·87	52·61	49·11	49·33
TiO_2	2·23	2·71	0·79	0·54	0·66	0·58	1·27	2·23
Al_2O_3	7·10	9·59	7·56	11·38	10·96	11·62	15·84	13·94
Fe_2O_3*	16·32	16·88	12·36	10·96	14·06	10·95	11·93	15·13
MnO	0·23	0·17	0·19	0·19	0·23	0·19	0·19	0·22
MgO	15·27	12·8	17·24	10·84	8·51	10·79	6·31	5·67
CaO	7·70	6·67	8·21	9·04	8·71	9·18	11·33	9·92
Na_2O	0·41	1·46	1·38	2·00	2·42	1·61	2·66	2·42
K_2O	2·80	2·25	0·42	1·40	1·41	1·19	0·65	0·50
P_2O_5	0·25	0·37	0·09	0·08	0·09	0·08	0·11	0·21
LOI	4·10	3·39	0·72	1·15	1·00	0·72	0·52	0·28
mg no.	65	60	73	66	55	66	51	43
Cr	1283	780	3634	859	846	790	271	109
Ni	963	544	724	224	202	215	80	71
Co	n.d.	n.d.	116	53	86	49	n.d.	81
Sc	29	26	n.d.	37	n.d.	35	n.d.	n.d.
V	279	287	239	199	186	208	284	381
Cu	259	76	60	29	55	77	78	228
Pb	<0·5	4	1	10	4	<4	4	8
Zn	n.d.	n.d.	72	104	184	100	111	137
Rb	99	92	10	103	29	62	4	4
Ba	355	741	62	265	223	213	112	53
Sr	34	150	97	96	162	134	199	211
Ga	16	21	13	12	14	12	18	22
Nb	21	19	4·8	<2	3·7	3	4·4	8·2
Hf	6	6	n.d.	<5	n.d.	<5	n.d.	n.d.
Zr	195	225	61	50	73	52	81	131
Y	24	29	12	n.d.	18	<3	23	30
Th	<3	3	0·5	<5	1·1	<5	0·5	0·8
U	0·5	<0·5	<0·5	<3	<0·5	<3	<0·5	<0·5
Latitude	−73·656	−73·651	−73·51533	−72·95383	−73·63050	−73·08283	−73·57923	−73·56905
Longitude	68·424	68·419	68·30817	66·00500	68·37000	66·26933	68·34504	68·36253
Lab.	1	1	2	3	2	3	2	2

(continued)

uncommon, largely west-trending, but sometimes NE- or SE-trending, dykes encountered in the southern Mawson Escarpment and in Mts Stinear and Rymill. The rocks of subalkaline tholeiitic composition make up the majority of the mafic dykes (NNE-, NW-, and ENE-trending) observed within the Ruker Complex, whereas the high-Ti–P metabasites are sills found within the Sodruzhestvo Group.

Table 1: Continued

Sample ID:	sPCM 71.3	9828167	sPCM 71.1	9828191	9828200	9828202	9828199	9828054	9828196
Locality:	McCue Bluff	Tingey Glacier	McCue Bluff	McCue Bluff	McCue Bluff	McCue Bluff	McCue Bluff	Rimmington Bluff	McCue Bluff
Suite:[1]	NNE	NNE	NNE	NNE	NNE	NW	NW	NW	NW
Group:	Low-LILE	Low-LILE	Low-LILE	Low-LILE	Low-LILE	High-LILE	High-LILE	High-LILE	High-LILE
Rock:	Dolerite	Mafic schist	Dolerite	Metadolerite	Dolerite	Altered dolerite	Amphibolite	Mafic schist	Altered dolerite
SiO_2	49·59	49·73	49·73	50·07	50·42	46·2	46·64	49·6	53·23
TiO_2	2·13	1·48	2·18	0·97	2·16	2·18	1·31	2·25	1·59
Al_2O_3	12·88	14·00	12·95	14·25	13·19	14·08	15·24	12·98	13·11
Fe_2O_3*	16·13	15·22	16·19	11·44	15·48	16·91	14·13	15·63	15·91
MnO	0·26	0·22	0·25	0·19	0·22	0·21	0·19	0·21	0·18
MgO	5·78	6·06	5·59	7·67	5·87	5·71	7·25	5·15	3·74
CaO	10·18	10·18	10·2	10·82	10·26	8·89	9·97	9·24	7·94
Na_2O	2·34	2·08	2·30	2·85	2·23	2·41	2·26	2·53	2·61
K_2O	0·36	0·34	0·36	0·70	0·39	1·09	0·63	1·23	1·52
P_2O_5	0·19	0·17	0·19	0·09	0·20	0·48	0·25	0·36	0·24
LOI	0·10	0·38	0·05	0·84	0·62	1·66	1·97	0·61	0·27
mg no.	42	44	41	57	43	40	50	39	32
Cr	130	144	127	257	180	58	149	141	30
Ni	70	83	66	99	59	74	110	74	53
Co	54	71	45	71	70	74	75	78	62
Sc	40	n.d.	40	n.d.	n.d.	n.d.	n.d.	n.d.	n.d.
V	368	408	370	291	347	262	215	304	343
Cu	220	86	210	22	249	64	78	187	135
Pb	<4	5	<4	9	1	6	5	3	8
Zn	128	131	129	125	115	150	103	133	109
Rb	10	2	12	8	8	25	15	39	61
Ba	170	71	173	32	93	651	362	208	390
Sr	175	254	173	178	174	244	247	124	153
Ga	23	19	22	15	22	21	17	18	20
Nb	6	11·5	6	3·5	7·8	22·9	15·6	14·7	9·6
Hf	<5	n.d.	<5	n.d.	n.d.	n.d.	n.d.	n.d.	n.d.
Zr	154	103	161	56	147	208	115	244	169
Y	24	22	26	18	35	32	20	52	39
Th	<5	1·2	<5	0·4	1·3	3·1	1·3	6·5	6
U	<3	<0·5	<3	<0·5	<0·5	<0·5	<0·5	0·9	0·6
Latitude	−73·51083	−73·53600	−73·51083	−73·52550	−73·50950	−73·50950	−73·51533	−73·57923	−73·52550
Longitude	68·31433	68·31283	68·31433	68·31133	68·30433	68·30433	68·30817	68·34504	68·31133
Lab.	3	2	3	2	2	2	2	2	2

(continued)

High-Mg metabasite

These rocks, which vary in texture and composition from noritic metadolerite to mafic and ultramafic schist, have mg numbers largely between 55 and 73. They have either quartz–hypersthene (silica-oversaturated) or hypersthene–olivine normative CIPW compositions. Normative olivine is <2·2%, hypersthene is mostly between 18 and 35%. Modal anorthite content is generally low (10–20%). These rocks have characteristically high MgO (8–18 wt %), Cr (800–3600 ppm) and Ni (200–960 ppm) contents, low concentrations of Al_2O_3 (mostly <13 wt %), and high CaO/Al_2O_3 ratios (0·7–1·1). They also tend to

Table 1: Continued

Sample ID:	sPCM 64.3	9828214	48159-13	9828192	sPCM 73.4	9828157	sPCM 69.5	sPCM 80.1	sPCM 28.1
Locality:	Tingey Glacier	McCue Bluff	McCue Bluff	McCue Bluff	McCue Bluff	Tingey Glacier	Rimmington Bluff	Binders Nunataks	Mt Stinear
Suite:[1]	ENE	ENE	ENE	ENE	ENE	ENE	ENE		
Group:	Low-LILE	Low-LILE	Low-LILE	High-LILE	High-LILE	High-LILE	High-LILE	Low-LILE	High-LILE
Rock:	Metadolerite	Dolerite	Dolerite	Amphibolite	Amphibolite	Amphibolite	Metadolerite	Amphibolite	Metadolerite
SiO_2	49·46	49·66	49·68	48·97	49·29	50·05	52·64	49·06	49·22
TiO_2	1·25	1·71	2·30	2·44	1·96	1·50	0·70	2·41	0·97
Al_2O_3	14·03	13·66	13·04	13·04	11·98	13·72	13·84	12·54	14·51
Fe_2O_3*	13·43	15·59	16·44	15·91	14·91	16·11	12·03	17·19	12·38
MnO	0·20	0·21	0·23	0·21	0·22	0·21	0·19	0·25	0·24
MgO	6·55	5·89	5·42	5·06	5·34	6·12	6·13	5·45	7·43
CaO	11·05	9·93	9·84	9·54	8·61	9·11	10·22	9·76	10·56
Na_2O	2·54	2·52	2·31	2·05	1·31	0·73	2·47	1·96	2·49
K_2O	0·28	0·39	0·42	1·62	4·26	0·97	0·83	0·57	1·11
P_2O_5	0·14	0·22	0·21	0·36	0·18	0·17	0·10	0·20	0·08
LOI	0·48	0·06	0·20	0·60	1·25	1·13	0·43	0·15	0·48
mg no.	49	43	40	39	41	43	50	40	54
Cr	269	224	107	133	131	157	32	36	271
Ni	100	75	73	65	68	153	101	64	152
Co	54	59	47	63	43	78	50	50	51
Sc	40	n.d.	38	n.d.	26	n.d.	40	46	42
V	268	290	364	308	309	418	238	402	267
Cu	149	161	217	152	20	114	65	233	23
Pb	<4	<0·7	<4	5	11	2	5	<4	13
Zn	101	122	131	123	191	87	102	141	328
Rb	10	11	8	38	89	21	16	11	39
Ba	94	81	113	180	661	264	245	173	123
Sr	141	136	177	103	118	80	167	164	120
Ga	17	19	19	19	20	20	16	25	17
Nb	2	6	14	13·4	6	13	3	5	3
Hf	<5	n.d.	<5	n.d.	<5	n.d.	n.d.	<5	5
Zr	86	104	164	247	133	107	76	148	56
Y	17	34	41	57	19	26	13	23	9
Th	<5	0·5	<5	5·7	<5	2·6	<5	<5	<5
U	<3	<0·5	<3	0·8	<3	<0·5	<3	6	<3
Latitude	−73·54683	−73·50183	−73·511	−73·52540	−73·51467	−73·53767	−73·58050	−72·57300	−73·08517
Longitude	68·33167	68·31217	68·336	68·31133	68·31333	68·31750	68·34450	62·66683	66·26467
Lab.	3	2	3	2	3	2	3	3	3

(continued)

have lower TiO_2 concentrations (0·3–0·8 wt %) than the more common tholeiites. Mantle-normalized trace element patterns for these rocks are spiked, characterized by pronounced negative Nb anomalies. Two rocks additionally display negative Sr anomalies (Fig. 10a). These samples additionally have the highest concentrations of HFSE and also have noticeably higher Ti/Y and Zr/Y ratios. The mg numbers of these two rocks lie within the common range observed for this suite. A single sample from this suite was analysed for REE (Table 2) and has REE concentrations 8–11 times chondrite (Fig. 11a) with a slightly fractionated trend between the LREE and middle

Table 1: Continued

Sample ID:	sPCM 31.1	sPCM 51.1	sPCM 45.1	sPCM 51.2	sPCM 45.2	19-L[2]
Locality:	Mt Stinear	Cumpston Massif east	Cumpston Massif east	Cumpston Massif east	Cumpston Massif east	Mt Seddon
Suite:[1]		sill	sill	sill	sill	sill
Group:	Low-LILE	High-Ti–P	High-Ti–P	High-Ti–P	High-Ti–P	High-Ti–P
Rock:	Mafic schist	Amphibolite	Amphibolite	Amphibolite	Amphibolite	Amphibolite
SiO_2	51·16	45·85	46·40	46·43	48·07	46·40
TiO_2	1·02	4·10	4·01	4·52	3·84	4·68
Al_2O_3	13·65	15·05	14·74	15·01	15·77	14·62
Fe_2O_3*	14·05	15·41	15·38	15·60	13·72	15·19
MnO	0·22	0·23	0·25	0·23	0·20	0·22
MgO	6·77	5·51	5·49	4·80	4·43	4·71
CaO	9·43	9·01	8·36	8·41	8·07	7·69
Na_2O	2·54	2·84	3·13	2·92	3·56	3·12
K_2O	0·33	0·44	0·21	0·19	0·84	1·19
P_2O_5	0·08	1·02	1·03	1·10	0·96	1·30
LOI	0·31	0·04	0·49	0·30	0·06	1·60
mg no.	49	41	41	38	39	40
Cr	135	71	77	72	62	n.d.
Ni	105	45	42	28	31	n.d.
Co	58	50	50	41	48	n.d.
Sc	46	27	29	31	28	n.d.
V	286	123	108	119	94	n.d.
Cu	58	<10	12	22	12	n.d.
Pb	<4	10	26	29	11	n.d.
Zn	97	174	175	186	163	n.d.
Rb	9	14	7	7	18	n.d.
Ba	59	281	188	186	537	n.d.
Sr	167	269	302	340	342	n.d.
Ga	16	25	24	26	26	n.d.
Nb	6	15	18	16	15	n.d.
Hf	<5	5	8	12	7	n.d.
Zr	56	343	338	366	320	n.d.
Y	13	42	44	43	39	n.d.
Th	<5	<5	<5	<5	<5	n.d.
U	<3	<3	6	<3	<3	n.d.
Latitude	−73·09600	−73·60400	−73·57550	−73·60400	−73·57550	−73·118
Longitude	66·23867	66·97350	66·96350	66·97350	66·96350	64·930
Lab.	3	3	3	3	3	–[2]

[1]When specified.
[2]From Ravich *et al*. (1985), by wet chemistry.
*Total Fe as Fe_2O_3.
Major components in wt %, trace elements in ppm. LOI, loss on ignition; n.d., no data; Lab., laboratory [1, BMR (Canberra); 2, University of Melbourne; 3, BGR (Hannover)]. Sill indicates sills within the Neoproterozoic Sodruzhestvo Group. mg number = $100MgO/(MgO + FeO^{tot})$, mol %.

Table 2: REE concentrations (ppm) in mafic intrusive rocks from the southern Prince Charles Mountains

Sample	Locality	Geochemical group	Dyke suite or sill	La	Ce	Pr	Nd	Sm	Eu	Gd	Tb	Dy	Ho	Er	Tm	Yb	Lu	$(La/Yb)_N$
sPCM 29.1	Mt Rymill	High-Mg	E–W	6·33	13·5	1·76	7·34	1·91	0·63	1·91	0·37	2·04	0·46	1·38	0·20	1·30	0·20	3·50
sPCM 30.7	Mt Stinear	Low-LILE	NNE	8·43	21·2	3·12	15·1	4·38	1·33	4·36	0·76	4·36	0·88	2·36	0·35	2·01	0·31	3·00
sPCM 49.1	Cumpston M.	Low-LILE	NNE	4·18	9·77	1·40	6·55	1·91	0·74	2·26	0·43	2·71	0·60	1·69	0·25	1·64	0·26	1·80
9828200	McCue Bluff	Low-LILE	NNE	11·2	25·9	3·74	17·8	5·80	1·67	5·29	1·06	5·84	1·22	3·61	0·46	3·00	0·43	2·70
9828191	McCue Bluff	Low-LILE	NNE	3·93	10·0	1·46	7·44	2·20	0·84	2·53	0·50	2·97	0·57	1·87	0·24	1·58	0·24	1·80
9828054	Rimmington Bluff	High-LILE	NW	44·4	86·3	8·84	32·9	8·41	1·78	8·39	1·52	8·96	1·74	5·88	0·79	5·12	0·83	6·20
9828202	McCue Bluff	High-LILE	NW	46·2	89·0	10·1	37·1	7·42	2·09	6·75	1·07	5·66	1·16	3·38	0·46	2·91	0·42	11·4
9828214	McCue Bluff	Low-LILE	ENE	8·21	20·3	2·96	13·9	4·12	1·43	4·76	0·93	5·68	1·20	3·74	0·51	3·52	0·51	1·70
9828192	McCue Bluff	High-LILE	ENE	13·4	35·5	5·28	24·4	7·31	1·85	7·65	1·42	8·79	1·96	5·97	0·84	5·74	0·83	1·70
sPCM 51.1	Cumpston M.	High-Ti–P	sill	28·3	57·8	8·32	38·6	9·58	2·60	9·22	1·54	9·30	1·81	5·28	0·68	4·55	0·75	4·50
sPCM 52.5	Cumpston M.	High-Ti–P	sill	29·0	64·6	8·86	41·4	9·37	2·75	10·0	1·52	9·09	1·70	5·30	0·71	4·51	0·62	4·60
sPCM 44.2	Cumpston M.	High-Ti–P	sill	24·2	57·8	7·86	35·8	9·49	2·40	10·3	1·71	9·20	1·83	5·19	0·69	4·11	0·69	4·20
sPCM 45.1	Cumpston M.	High-Ti–P	sill	27·5	60·5	8·13	40·4	9·78	2·82	9·35	1·49	8·84	1·71	5·21	0·63	4·49	0·70	4·40

REE (MREE; La–Gd) and a flat distribution for the heavy REE (HREE; Dy–Lu). The chondrite-normalized ratios of La_N/Yb_N and Gd_N/Yb_N are 3·49 and 1·22, respectively.

Subalkaline tholeiite

Two chemically distinct subalkaline tholeiitic rock groups can be distinguished: a low-LILE group and high-LILE group. Dykes of the NNE-trending suite compositionally lie within the low-LILE group, whereas those of the NW-trending suite (with one exception) lie within the high-LILE group. The ENE-trending suite is more heterogeneous and contains examples that fall within both geochemical groups.

NNE-trending dykes (low-LILE)

The NNE-trending dykes in the southern Mawson Escarpment define a coherent cluster with minor variations in terms of major and trace element abundances. Major element concentrations are $SiO_2 = 49–50·5$ wt %, $TiO_2 = 1·0–2·2$ wt %, $MgO = 5·0–7·7$ wt %, $Na_2O = 2·1–2·8$ wt %, $K_2O = 0·40–0·70$ wt % and $P_2O_5 = 0·10–0·20$ wt %. Mg number varies between 40 and 57. Mean concentrations of some trace elements are as follows (ppm): Rb 7, Ba 72, Nb 8·8, Sr 201, Zr 114, and Y 27. These dykes display relatively flat to slightly humped trace element patterns with no significant Nb or Sr anomaly. Most trace element concentrations are between five and 20 times mantle values, although normalized Pb concentrations are somewhat higher (Fig. 10b). The chondrite-normalized REE patterns are mostly flat, although a slight LREE enrichment in the more evolved samples is evident ($La_N/Yb_N = 2·7$ and 3·0; Fig. 11b). These rocks show some systematic differences when compared with dykes of the other suites. They tend to have somewhat lower concentrations of K, Rb, Ba, Th, La and Ce, and higher Cr. Less evident is their relative depletion in HFSE: P, Nb, and Zr.

NW-trending dykes (high-LILE)

Major element concentrations for the NW-trending suite are $SiO_2 = 46–56$ wt %, $TiO_2 = 0·6–2·3$ wt %, $MgO = 2·4–7·3$ wt %, $Na_2O = 2·1–2·5$, $K_2O = 0·6–2·2$ wt % and $P_2O_5 = 0·10–0·60$ (Table 1). Mg number varies between 24 and 55. Mean trace element concentrations are as follows: Rb 39 ppm, Ba 295 ppm, Nb 11·2 ppm, Sr 140 ppm, Zr 188 ppm, and Y 34 ppm. These rocks show mostly overlapping major element concentrations with the NNE suite (Figs 6–8). The exceptions are K_2O, which is higher in most samples, and SiO_2, which varies more widely. More pronounced differences are observed in the trace element concentrations. Apart from prominent LILE enrichment—Rb_N and Ba_N are in the range 20–150 (Fig. 10c)—these rocks have, with few exceptions, prominent negative Nb and Sr anomalies and elevated LREE abundances (Fig. 11c). La_N/Yb_N is between 6·2 and 11·4.

ENE-trending dykes

The ENE-trending dykes tend to be more heterogeneous and contain rocks with characteristics akin to both the low-LILE group and the high-LILE group rocks. This is best expressed in the normalized trace element patterns shown in Fig. 10d. The studied ENE-trending dykes are all

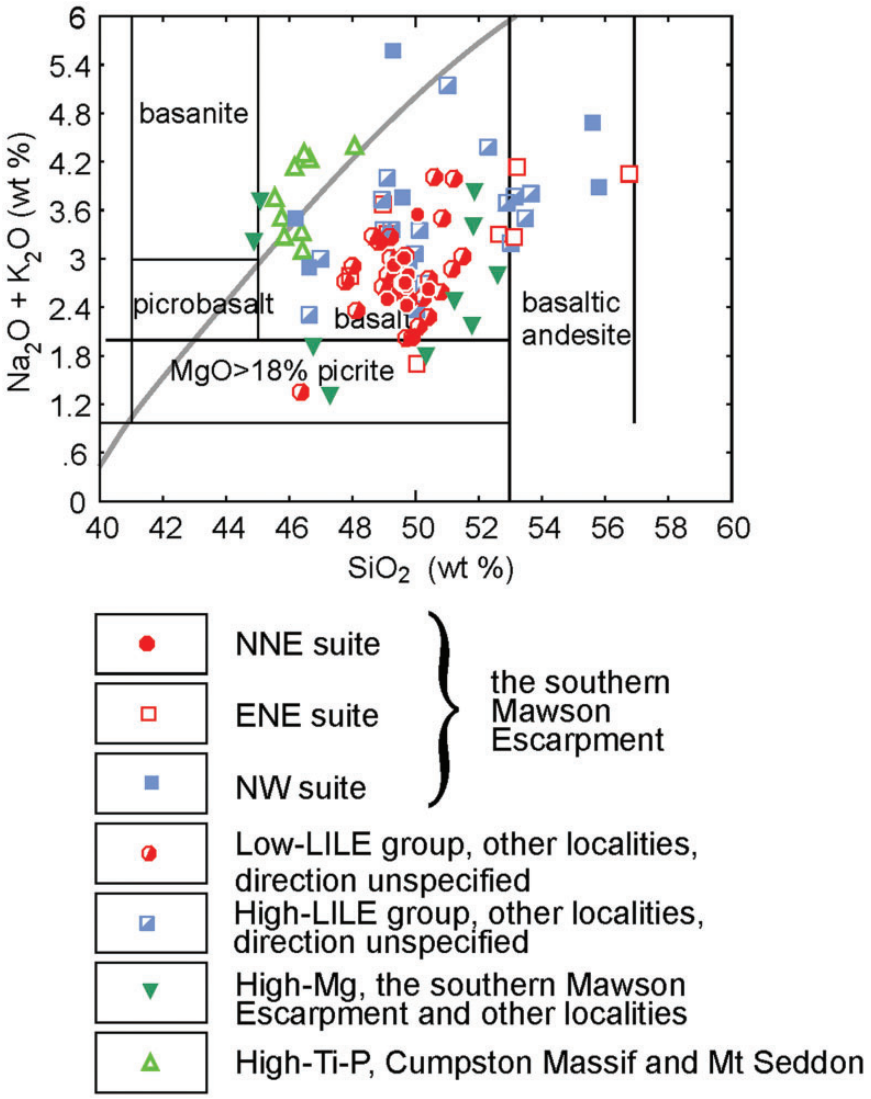

Fig. 6. A SiO_2–total alkalis classification diagram (Le Maitre, 1989) for mafic intrusions from the southern Prince Charles Mountains. Grey line divides alkaline and sub-alkaline rocks.

strongly evolved (mg number = 30–44) and most trace element ratios, especially those including the HFSE (e.g. Zr/Y, Ti/Zr, Ti/P, K/Nb, Rb/Sr; Table 3), for low-LILE rocks from the ENE suite are nearly identical to the NNE dyke rocks. On the other hand, K/Rb and La/Nb ratios in the low-LILE ENE-trending dyke rocks are lower, although the REE patterns (Fig. 11d) for these rocks are very similar to those of the NNE-trending dykes. The high-LILE rocks from the ENE-trending dykes have mostly very similar trace element ratios to the NW-trending dykes (e.g. Ba/Nb, Ti/Zr, Zr/Y, Th/Nb, Ti/P, and Rb/Sr; Table 3). Other trace element ratios are somewhat different (e.g. P/Zr, Th/U and Ce/Y are lower, and K/Nb, K/Zr and Zr/Nb are higher), suggesting derivation from somewhat different sources.

Unspecified dykes from other localities

Dyke rocks geochemically corresponding to either the low-LILE or high-LILE group have been found at other localities in the sPCM. The low-LILE dyke rocks are abundant in Mt Stinear. These dykes are variously fractionated (mg number = 40–54), as are the NNE-trending dykes in the southern Mawson escarpment. The low-LILE rocks from Mt Stinear show some trace elements ratios (e.g. La/Nb, Ti/P, P/Zr, Ti/Zr, La/Nb, Rb/Sr; Table 3) similar to those of the NNE-trending dykes, but many other ratios are very different (e.g. K/Rb and K/Nb are lower, and Zr/Nb, Ba/Nb and Zr/Y are higher). This indicates essential differences in the composition of their mantle sources and/or influences of different processes during magma ascent and within the upper crust during crystallization.

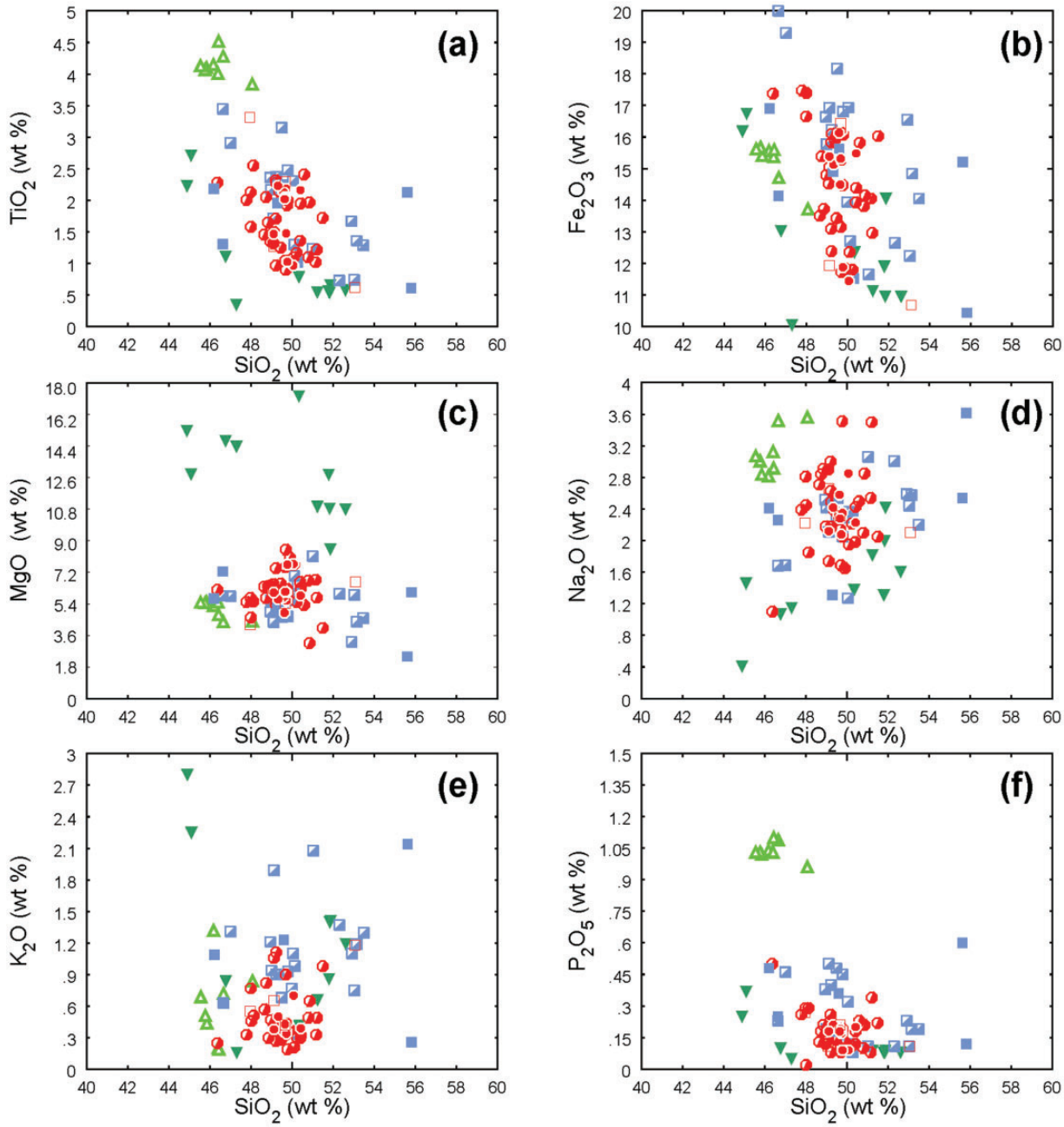

Fig. 7. SiO_2 vs major oxide components plots for mafic intrusions from the southern Prince Charles Mountains. Symbols as in Fig. 6.

The high-LILE group rocks, which occur elsewhere in the sPCM, have major element concentrations in the following ranges: $SiO_2 = 46–53$ wt %, $TiO_2 = 0·7–3·1$ wt %, $MgO = 3·2–8·1$ wt %, $Na_2O = 0·7–3·1$, $K_2O = 0·6–2·1$ wt % and $P_2O_5 = 0·10–0·50$ wt %. These compositional ranges closely correspond to the high-LILE group dykes from the Mawson Escarpment. Scatter in trace element contents is also limited, with mean concentrations of Rb 41 ppm, Ba 410 ppm, Nb 16·3 ppm, Sr 182 ppm, Zr 206 ppm, and Y 40 ppm for the high-LILE group elsewhere in the study area, which is similar to the trace elements concentrations in the NW-trending suite in the Mawson Escarpment. The high-LILE rocks from Mt Stinear have nearly identical trace element ratios compared with the high-LILE ENE dykes in the Mawson Escarpment (Table 3).

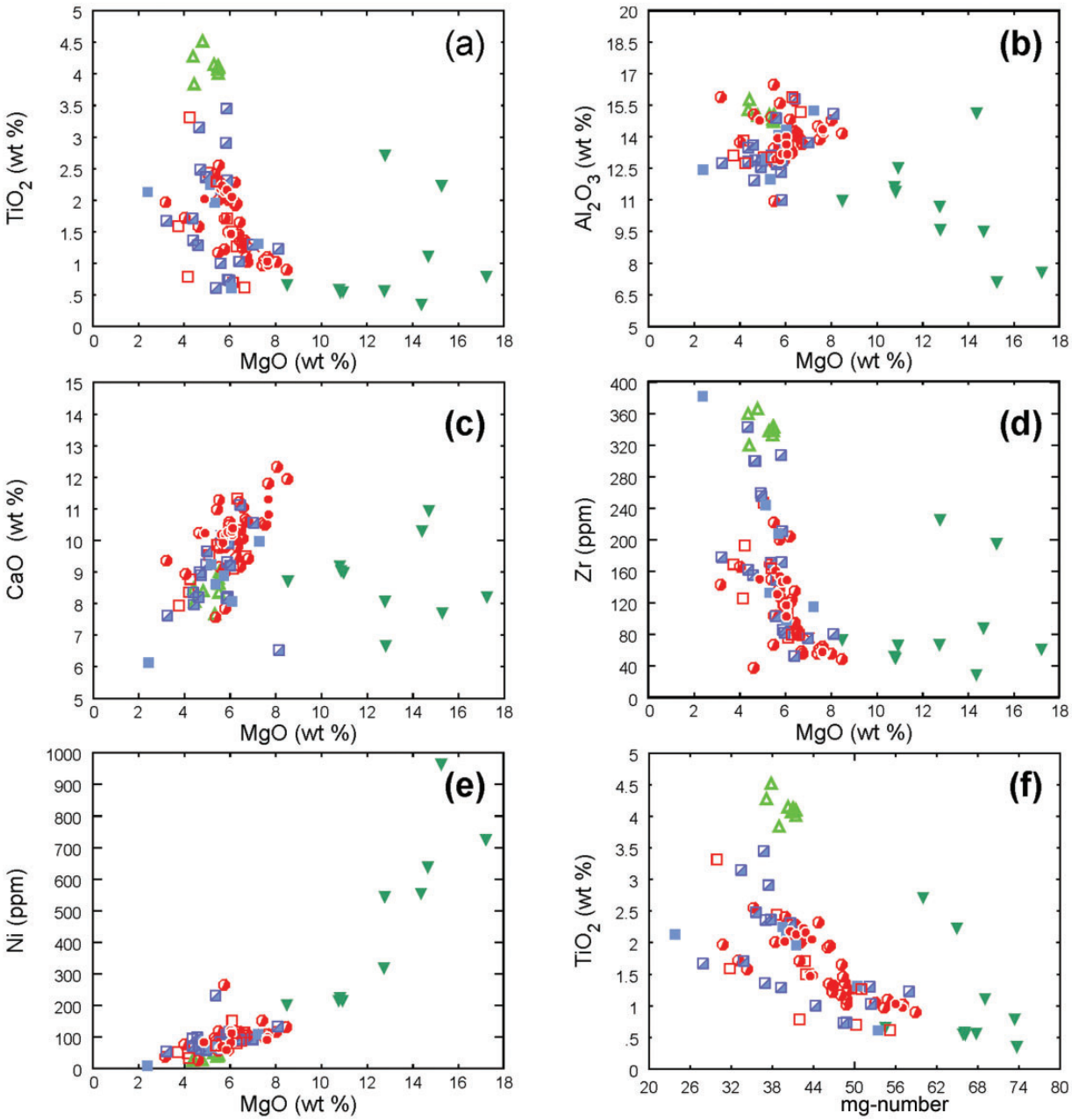

Fig. 8. Selected MgO, and mg number vs major and trace elements plots for mafic intrusions from the southern Prince Charles Mountains. Symbols as in Fig. 6.

High-Ti–P metabasite

High-Ti–P mafic compositions are restricted to sills in the Neoproterozoic metasediments of the Sodruzhestvo Group at Cumpston Massif (Phillips *et al.*, 2005) and Mt Seddon (Ravich *et al.*, 1985). These rocks have a relatively narrow range of concentrations for most major and trace elements. They have typically high TiO_2 (3·8–4·5 wt %) and P_2O_5 (0·96–1·10 wt %) and relatively low SiO_2 (46–48 wt %), Na_2O (2·8–3·5 wt %), Cr (60–85 ppm), Ni (30–50 ppm), V (90–120 ppm) and Cu (<20 ppm). MgO concentrations (4·4–5·5 wt %) are slightly lower than observed in the high-Mg and tholeiitic dykes. The abundances of K_2O, Pb, Rb, and Ba vary widely. These rocks are highly evolved (mg number = 37–41) and are silica-oversaturated, as indicated by normative quartz (4–8%) and hypersthene (11–14%) despite their low SiO_2 contents. They also tend to have higher Sr (mostly 300–340 ppm), Ga (22–26 ppm), Nb (15–18 ppm),

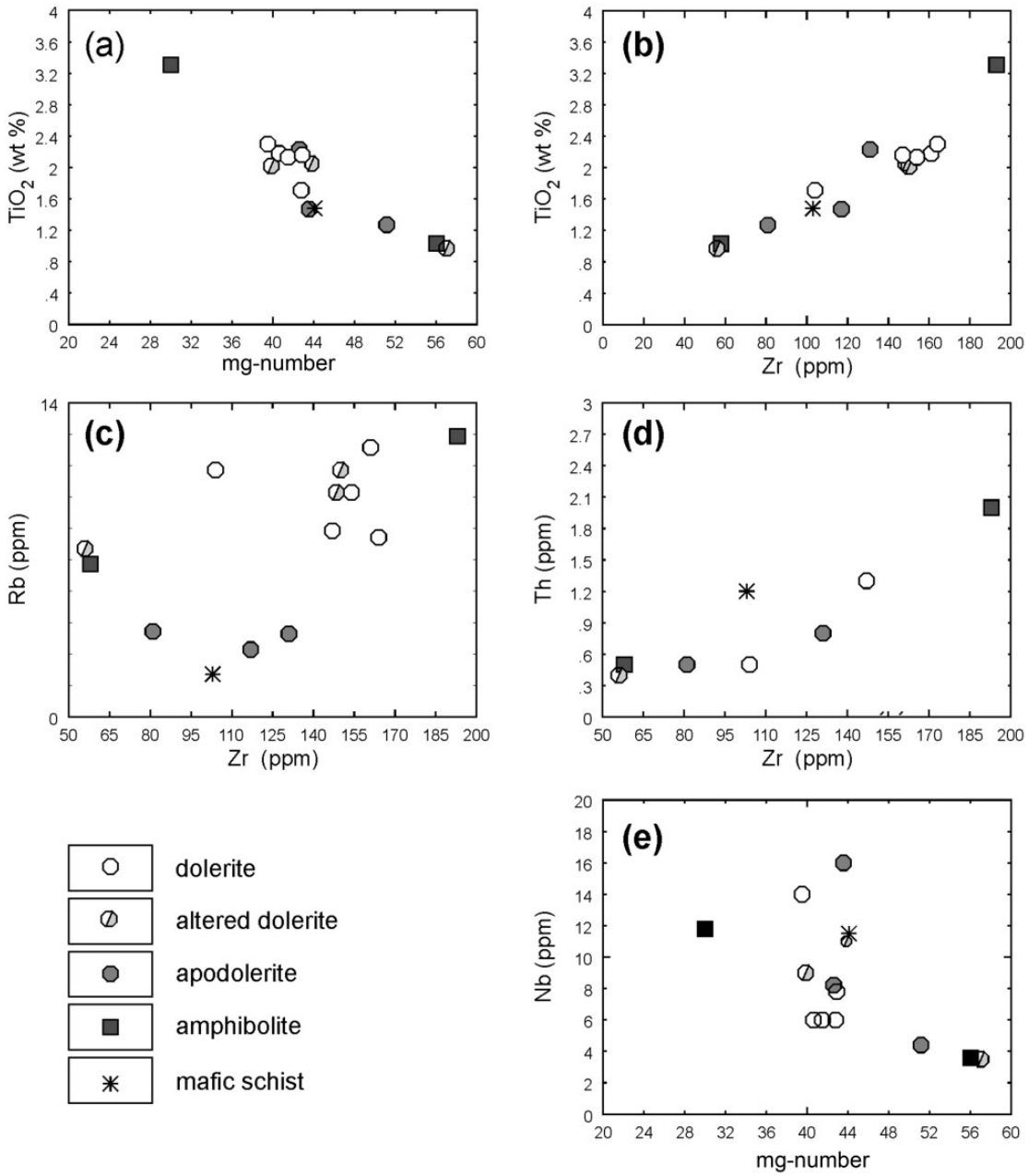

Fig. 9. Selected major and trace element variation diagrams for variously metamorphosed rocks.

and Zr (320–360 ppm) than either the tholeiitic or high-Mg dykes.

When normalized to primitive mantle (Fig. 10e), the high-Ti–P rocks show very consistent and relatively smooth trace element patterns (except K and Pb). They show prominent enrichment in the least incompatible HFSE elements, which results in a steep negative slope from P to Y. LILE are moderately enriched, but display considerable variations (particularly K_2O and Pb) that are probably due to alteration. Nb either shows no anomaly or defines a small negative anomaly. A prominent negative Sr anomaly is also present. Four samples were analysed for REE and these show consistent, slightly fractionated REE patterns ($La_N/Yb_N = 4{\cdot}2–4{\cdot}6$; Fig. 11a). A small negative Eu anomaly [$Eu^* = 0{\cdot}74–0{\cdot}89$, where $Eu^* = 2Eu_N/(Sm_N + Gd_N)$] is also observed.

Sm–Nd ISOTOPE SYSTEMATICS

Twenty-six samples were analyzed for their Sm–Nd isotope compositions (Table 4). They show considerable

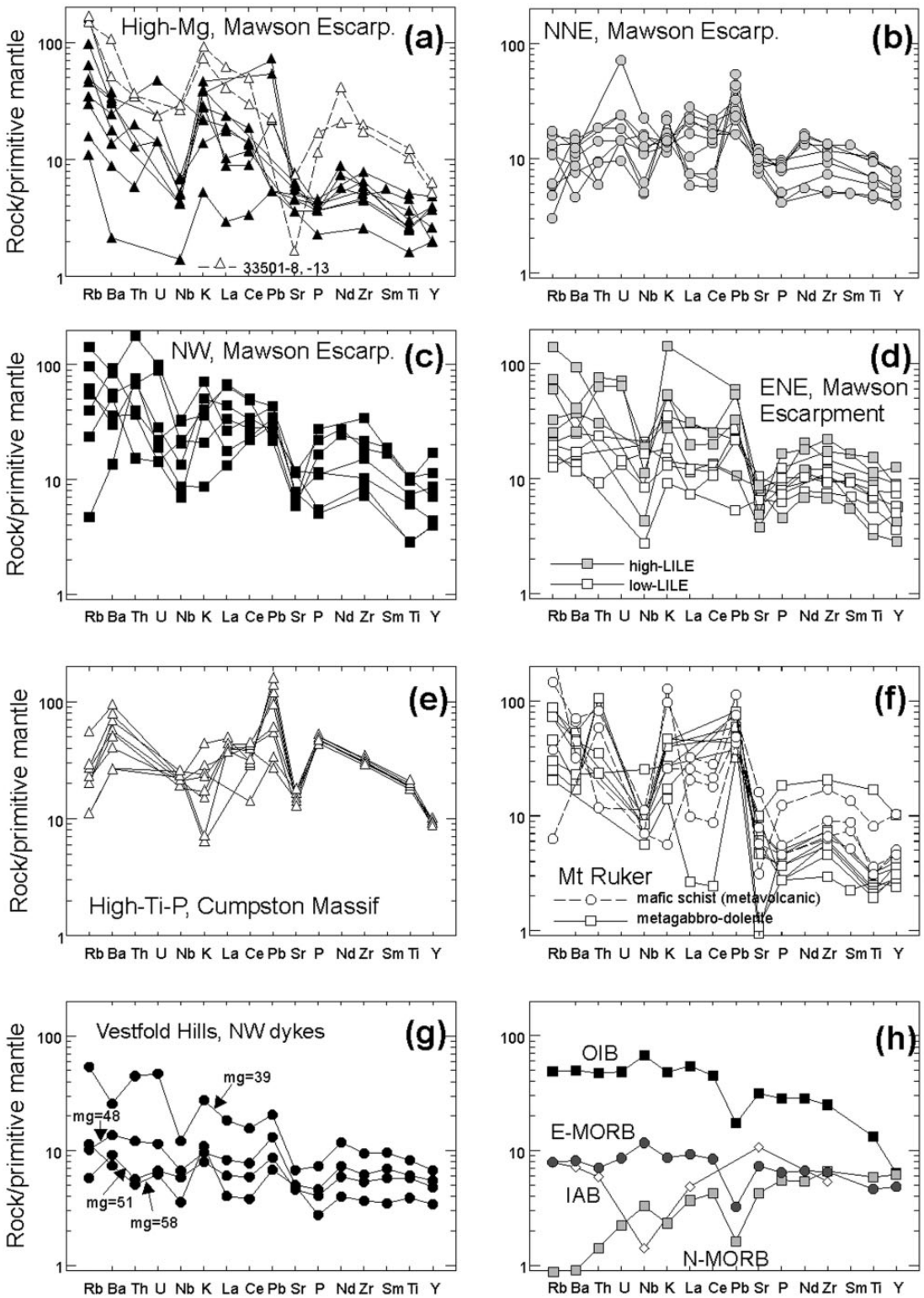

Fig. 10. Primitive mantle normalized trace element patterns for mafic intrusions from the southern Prince Charles Mountains. (a) High-Mg group, the southern Mawson Escarpment, Mts Stinear and Rymill. (b) NNE-trending dykes, the southern Mawson Escarpment. (c) NW-trending dykes, the southern Mawson Escarpment. (d) ENE-trending dykes, the southern Mawson Escarpment. (e) High-Ti–P sills intruding the Sodruzhestvo Group in Cumpston Massif. (f) Mafic schists (metavolcanics) and metagabbro–dolerites from the Ruker Group (Mikhalsky *et al.*, 2001; E. V. Mikhalsky, unpublished data). (g) NW-trending dykes from the Vestfold Hills (E. V. Mikhalsky, unpublished data). (h) Typical mantle-derived magmas after Sun & McDonough (1989) for comparison. Normalization factors from Sun & McDonough (1989). Island arc basalt (IAB) from Condie (1989). OIB, ocean island basalts; E-MORB, enriched mid-ocean ridge basalts; N-MORB, normal mid-ocean ridge basalts.

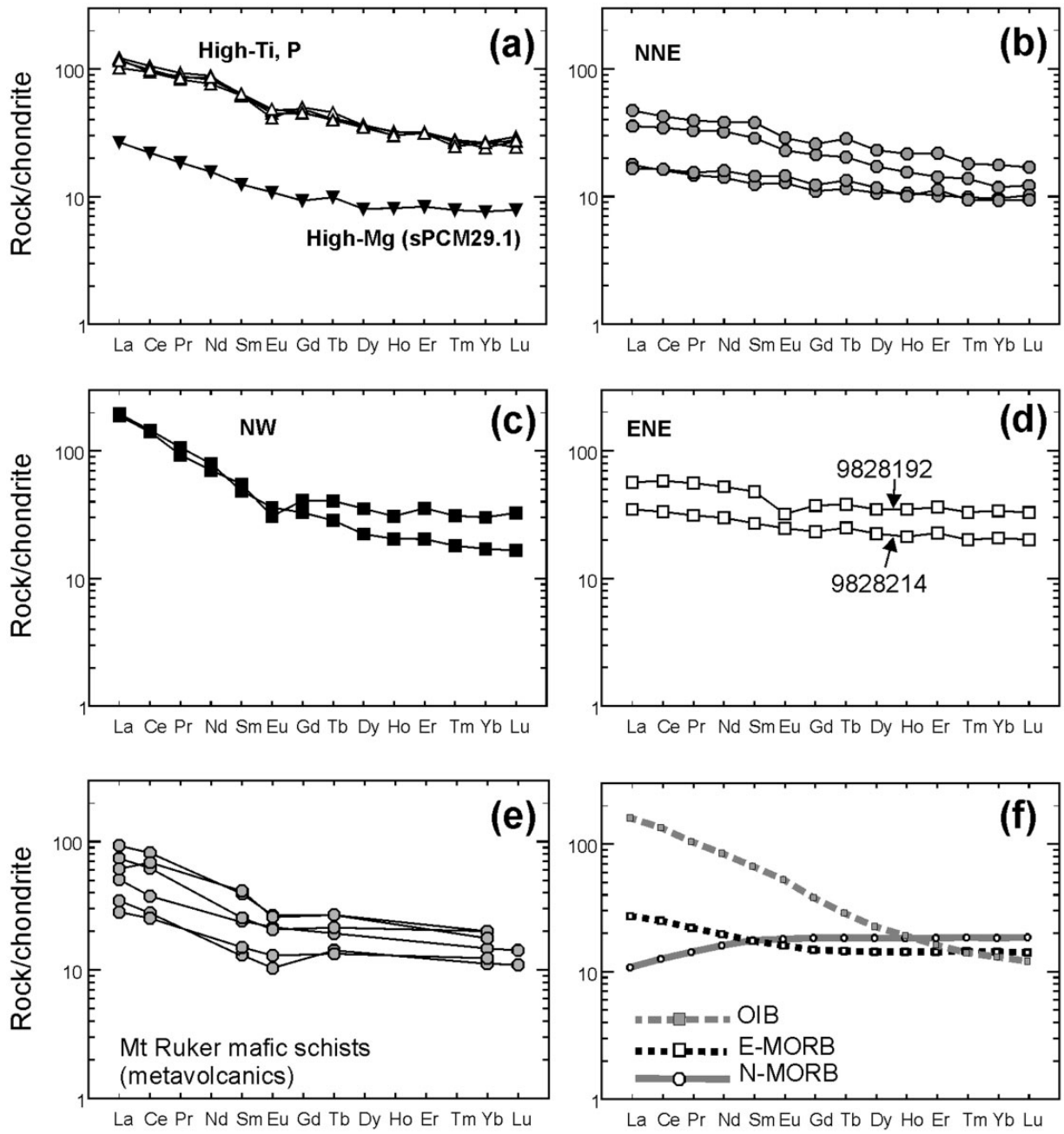

Fig. 11. Chondrite-normalized REE patterns for mafic intrusions from the southern Prince Charles Mountains. (a) High-Mg and high-Ti–P suites. (b) NNE-trending suite. (c) NW-trending suite. (d) ENE-trending suite. (e) Mafic schists (metavolcanic rocks) from the Ruker Group (data from Mikhalsky *et al.*, 2001). Normalization factors from Sun & McDonough (1989). N-MORB, E-MORB and OIB compositions (Sun & McDonough, 1989) are shown in (f) for comparison.

scatter in isotopic ratios and calculated parameters ε_{Nd} and depleted mantle model age $T_{DM}^{Sm/Nd}$ (T_{DM} below). For all analyzed rocks, $\varepsilon_{Nd}(0)$ varies between −0·5 and −23 with T_{DM} model ages of between 1660 and 3850 Ma. There are, however, systematic variations when the data are considered separately for the five suites of mafic intrusions.

Two samples of the high-Mg suite were analysed, and these reveal large negative $\varepsilon_{Nd}(0)$ values of −15·6 and −14·7, $f^{Sm/Nd}$ of −0·18 and −0·23 (see Table 4 for explanation), and T_{DM} model ages of 3·1 and 3·6 Ga. Taking 2370 Ma as the possible age of this suite [a TIMS date reported by Mikhalsky *et al.* (1992) and similar ages for high-Mg dykes in the Vestfold Hills reported by Collerson

Table 3: Selected average incompatible element ratios of subalkaline tholeiitic basites in the southern Prince Charles Mountains

Ratio	Mawson Escarpment				Mt Stinear		Mt Ruker*		
	NNE low-LILE	ENE low-LILE	ENE high-LILE	NW high-LILE	low-LILE	high-LILE	Mafic dykes	Mafic schists	Metagabbro-dolerites
Ti/P	14·5	13·3	10·6	7·3	14·4	10·4	11·9	11·2	9·7
P/Zr	6·3	6·9	6·1	7·5	6·4	6·4	5·5	5·4	5·6
K/Rb	777	401	369	275	592	273	113	251	226
K/Nb	650	585	1387	910	492	1156	815	1780	1490
K/Zr	41	36	81	62	26	62	65	124	136
Ce/Y	0·9	0·7	(1·2)	1·9	1·6	0·9	1·4	1·3	0·4
Ba/Nb	12·8	10·8	37·8	30·2	19	17·1	n.d.	48	45
La/Nb	1·3	(0·9)	(1·4)	2·1	1·6	1·3	1·3	2·3	0·5
Ti/Zr	90	90	65	54	92	66	60	59	56
Ti/Y	380	387	350	279	518	376	300	256	233
Zr/Nb	15·7	13·3	18·0	13·9	21·3	18·8	11·1	14·2	11·1
Zr/Y	4·3	4·3	5·3	5·1	5·7	5·7	5·1	4·4	4·4
Th/U	(3·0)	(4·7)	(4·2)	7·1	n.d.	n.d.	n.d.	n.d.	n.d.
Th/La	(0·1)	(0·2)	(0·4)	0·3	n.d.	n.d.	n.d.	n.d.	n.d.
Th/Nb	(0·15)	(0·15)	(0·5)	0·4	n.d.	(0·4)	n.d.	1	1·1
Rb/Sr	0·04	0·06	0·35	0·26	0·03	0·50	0·6	0·7	0·3
n	10	5	5	7	6	6	6	15	6
	(6)	(2–4)	(3)		(2)	(3)			

*Mikhalsky *et al.* (2001); E. V. Mikhalsky, unpublished data.
n.d., no data.

& Sheraton (1986) and Lanyon *et al.* (1993)] gives initial $\varepsilon_{Nd}(2{\cdot}37)$ values of −2 and −4 (Fig. 12a). These data indicate an enriched mantle source for these rocks.

Twenty-two analyses were made of the subalkaline tholeiites and for each suite distinctive isotopic characteristics were observed. NNE-trending dykes (low-LILE group rocks; seven samples) have $\varepsilon_{Nd}(0)$ values between zero and −3, $f^{Sm/Nd}$ of −0·08 to −0·15, and T_{DM} of 1·9–2·5 Ga. One outlying sample has $\varepsilon_{Nd}(0) = -8{\cdot}4$ and $T_{DM} = 1{\cdot}7$ Ga. The slope in time–ε_{Nd} space for this rock is thus markedly steeper than for the other samples from this suite owing to significantly lower $f^{Sm/Nd} = -0{\cdot}34$ (Fig. 12b). Assuming a post-1·3 Ga and probably pre-1·0 Ga age for these dykes (see below) initial $\varepsilon_{Nd}(1{\cdot}0–1{\cdot}3)$ between zero and +2·5 may be calculated.

NW-trending dykes (high-LILE group rocks; four samples) yielded negative $\varepsilon_{Nd}(0)$ values between −12 and −23 and T_{DM} model ages between 2·3–2·9 Ga. The slope in time–$\varepsilon_{Nd}(0)$ space for these rocks is steep owing to low $f^{Sm/Nd} = -0{\cdot}30$ to −0·45 (Fig. 12c). The isotopic characteristics from this dyke suite are thus distinct from those of the NNE-trending dykes described above, and from those of the ENE-trending dykes described below.

ENE-trending dykes (seven samples) yield low $\varepsilon_{Nd}(0)$ between −2·8 and −20 and T_{DM} model ages of 2·3–3·85 Ga, although most values are between 2·9–3·85 Ga. $f^{Sm/Nd}$ is between −0·10 and −0·22 and the slope in time–$\varepsilon_{Nd}(0)$ space is thus relatively flat (Fig. 12d). Unlike the NW- or NNE-trending dykes that geochemically fall into either the high-LILE group (NW dykes) or the low-LILE group (NNE dykes), the ENE-trending dykes are compositionally mixed and composed of rocks with both low-LILE and high-LILE compositions. Although our dataset is small, the ENE-trending dykes with low-LILE group chemistry tend to have both the younger model ages between 2·3 and 3·4 Ga and higher $\varepsilon_{Nd}(0)$ between −2·8 and −7·8. For the high-LILE group rocks within this suite T_{DM} varies between 2·7 and 3·85 Ga and $\varepsilon_{Nd}(0)$ between −5·5 and −20·0. Only one sample (48159-13) of the low-LILE group of this suite has been tentatively dated at *c.* 1350–1300 Ma (Mikhalsky *et al.*, 2007). This sample gives initial $\varepsilon_{Nd}(1{\cdot}35) = +1{\cdot}7$. The

Table 4: Sm–Nd concentration and isotope data for mafic dykes and sills from the southern Prince Charles Mountains

Sample ID	Locality	Rock	Subalkaline tholeiite dyke suite	Geochem-ical group	Sm (ppm)	Nd (ppm)	$^{147}Sm/^{144}Nd$	$^{143}Nd/^{144}Nd$	$\varepsilon_{Nd}(0)$	T_{DM} (Ga)	$f^{Sm/Nd}$	Lab.
sPCM29.1	Mt Rymill	Mafic schist	E–W*	High-Mg	1·92	7·63	0·1514	0·511840	−15·6	3·19	−0·23	BGR
sPCM D	Mt Rymill	Apodolerite	E–W*	High-Mg	1·70	6·38	0·1607	0·511886	−14·7	3·61	−0·18	BGR
9828054	Rimmington Bluff	Mafic schist	NW	High-LILE	7·92	34·86	0·1371	0·511998	−12·5	2·29	−0·30	UniMelb
9828199	McCue Bluff	Amphibolite	NW	High-LILE	4·05	22·11	0·1107	0·511577	−20·7	2·32	−0·44	UniMelb
9828202	McCue Bluff	Altered dolerite	NW	High-LILE	7·28	40·57	0·1085	0·511415	−23·9	2·50	−0·45	UniMelb
9828196	McCue Bluff	Altered dolerite	NW	High-LILE	6·41	29·45	0·1315	0·511554	−21·2	2·95	−0·33	UniMelb
48159-13	McCue Bluff	Dolerite	ENE	Low-LILE	5·92	20·99	0·1706	0·512492	−2·8	2·33	−0·13	BGR
9828214	McCue Bluff	Dolerite	ENE	Low-LILE	4·32	15·24	0·1715	0·512224	−8·1	3·33	−0·13	UniMelb
sPCM64.3	Rimmington Bluff	Metadolerite	ENE	Low-LILE	3·16	10·76	0·1770	0·512334	−5·9	3·38	−0·10	BGR
sPCM73.4	McCue Bluff	Amphibolite	ENE	High-LILE	4·52	16·44	0·1655	0·512361	−5·4	2·49	−0·16	BGR
9828157	Tingey Glacier	Amphibolite	ENE	High-LILE	4·21	15·34	0·1657	0·512199	−8·6	3·01	−0·16	UniMelb
9828192	McCue Bluff	Amphibolite	ENE	High-LILE	7·34	26·14	0·1696	0·512047	−11·5	3·79	−0·14	UniMelb
sPCM69.5	Rimmington Bluff	Metadolerite	ENE	High-LILE	2·41	9·47	0·1534	0·511616	−19·9	3·85	−0·22	BGR
9828167	Tingey Glacier	Mafic schist	NNE	Low-LILE	4·17	19·39	0·1297	0·512192	−8·7	1·74	−0·34	UniMelb
9828038	Rimmington Bluff	Apodolerite	NNE	Low-LILE	5·02	18·05	0·1679	0·512564	−1·4	1·95	−0·15	UniMelb
sPCM71.3	McCue Bluff	Dolerite	NNE	Low-LILE	5·45	19·17	0·1713	0·512507	−2·6	2·31	−0·13	BGR
sPCM71.1	McCue Bluff	Dolerite	NNE	Low-LILE	5·51	19·38	0·1713	0·512496	−2·8	2·35	−0·13	BGR
9828200	McCue Bluff	Dolerite	NNE	Low-LILE	5·41	19·05	0·1717	0·512478	−3·1	2·44	−0·13	UniMelb
9828055	Rimmington Bluff	Apodolerite	NNE	Low-LILE	2·95	9·92	0·1794	0·512597	−0·8	2·46	−0·09	UniMelb
9828191	McCue Bluff	Metadolerite	NNE	Low-LILE	2·33	7·82	0·1800	0·512590	−0·9	2·53	−0·08	UniMelb
9828211	McCue Bluff	Altered dolerite	Undeterm.	Low-LILE	6·22	22·09	0·1702	0·512475	−3·2	2·36	−0·13	UniMelb
sPCM80.1	Binders Nts	Amphibolite	Undeterm.	Low-LILE	5·69	19·22	0·1789	0·512561	−1·5	2·58	−0·09	BGR
sPCM31.1	Mt Stinear	Mafic schist	Undeterm.	Low-LILE	2·51	8·82	0·1711	0·512329	−6·0	2·93	−0·13	BGR
sPCM28.1	Mt Stinear	Metadolerite	Undeterm.	Low-LILE	2·39	7·69	0·1869	0·512530	−2·1	3·52	−0·05	BGR
sPCM45.1	Cumpston Massif	Mafic schist†	–	High-Ti-P	9·84	41·82	0·1417	0·512364	−5·3	1·66	−0·28	BGR
sPCM51.1	Cumpston Massif	Amphibolite†	–	High-Ti-P	9·87	41·78	0·1422	0·512363	−5·4	1·68	−0·28	BGR

*Assigned to.
$f^{Sm/Nd} = (^{147}Sm/^{144}Nd_{sam})/(^{147}Sm/^{144}Nd_{CHUR}) - 1$.
†Sill; other rocks, dykes.
ε(Nd) calculated after DePaolo (1988) using the present-day values for a chondritic uniform reservoir (CHUR) $^{143}Nd/^{144}Nd = 0{\cdot}512638$ and $^{147}Sm/^{144}Nd = 0{\cdot}1967$ (Jacobsen & Wasserburg 1984); T_{DM} calculated after Goldstein & Jacobsen (1988) using $^{147}Sm/^{144}Nd_{DM} = 0{\cdot}2136$, $^{143}Nd/^{144}Nd_{DM} = 0{\cdot}513151$. UniMelb, University of Melbourne.

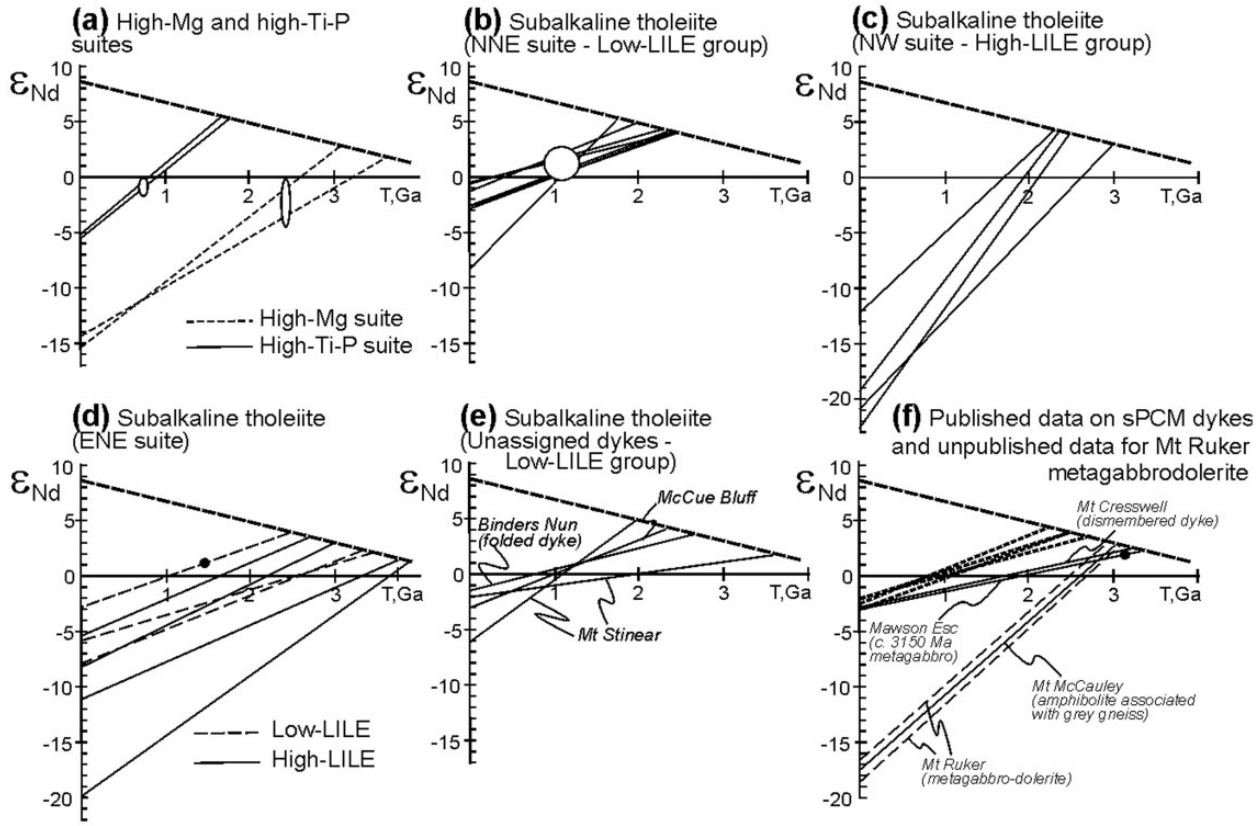

Fig. 12. Sm–Nd isotope evolution diagrams after DePaolo (1988). (a) High-Mg and high-Ti–P suites. (b–e) Subalkaline tholeiite suites: (b) NNE-trending dykes, low-LILE; (c) NW-trending dykes, high-LILE; (d) ENE-trending dykes; (e) unassigned direction dykes, low-LILE. (f) Other data for mafic rocks from the Ruker Complex: lines indicate various metabasites (Mikhalsky *et al.*, 2010); fine long-dash lines, metagabbro–dolerites in Ruker Group (E. V. Mikhalsky, unpublished data); bold short-dash line, NNE-trending mafic dykes in the southern Mawson Escarpment (Mikhalsky *et al.*, 1993). Initial Nd isotopic composition is indicated with a dot or ellipse, black when dated and white when assumed. Ages of ENE suite from Mikhalsky *et al.* (2007), metagabbro in Mawson Escarpment from Mikhalsky *et al.* (2010).

relatively large spread of T_{DM} model ages observed in this suite may be caused by rather high Sm/Nd ratios coupled with isotopic source heterogeneity and/or some crustal contamination.

Nd isotopic data were obtained for four dykes with unspecified strike but belonging to the low-LILE group rocks: one from McCue Bluff, two from Mt Stinear and one from Binders Nunataks (Fig. 12e). Three of the samples have $\varepsilon_{Nd}(0)$ values between −1·5 and −6·0 and T_{DM} values between 2·3 and 2·9 Ga. These data overlap with the range of $\varepsilon_{Nd}(0)$ and T_{DM} values obtained from the NNE-trending dykes and may indicate that these dykes belong to this suite. The remaining sample (from Mt Stinear) yielded a similar $\varepsilon_{Nd}(0)$ of −2, although the T_{DM} model age was considerably older (3·5 Ga). These results are more consistent with the data obtained from the low-LILE group rocks assigned to the ENE suite.

The high-Ti–P suite from Cumpston Massif (two samples analyzed) have relatively low $f^{Sm/Nd}$ of −0·28, $\varepsilon_{Nd}(0)$ values of −5·3, and T_{DM} of *c.* 1·6 Ga. Assuming the age of this suite to be <970 Ma (Phillips *et al.*, 2006) gives initial values of $\varepsilon_{Nd}(0{\cdot}9–0{\cdot}5\,Ga)$ of between zero and −3. These features confirm the distinctive geochemical signature of these rocks when compared with the dyke suites that intrude the older basement of the Ruker Complex.

PETROGENETIC CONSTRAINTS

High-Mg metabasites

The high-Mg metabasite dykes from the Ruker Complex have high concentrations of MgO, Cr and Ni, and low TiO_2, Al_2O_3, Na_2O, P, Zr and Nb, features that are characteristic of siliceous high-Mg basalts (e.g. Crawford *et al.*, 1989). High MgO, Cr and Ni, along with high mg numbers (up to 73), suggest that these rocks formed by a large degree of partial melting of their mantle source. Compositional variations in the mantle source, fractional crystallization and/or assimilation processes may be responsible for the observed chemical heterogeneity. In addition, the poor correlation between Zr and mg number (Fig. 13a) suggests that the compositional variations may also be due to varying degrees of partial melting: a lower

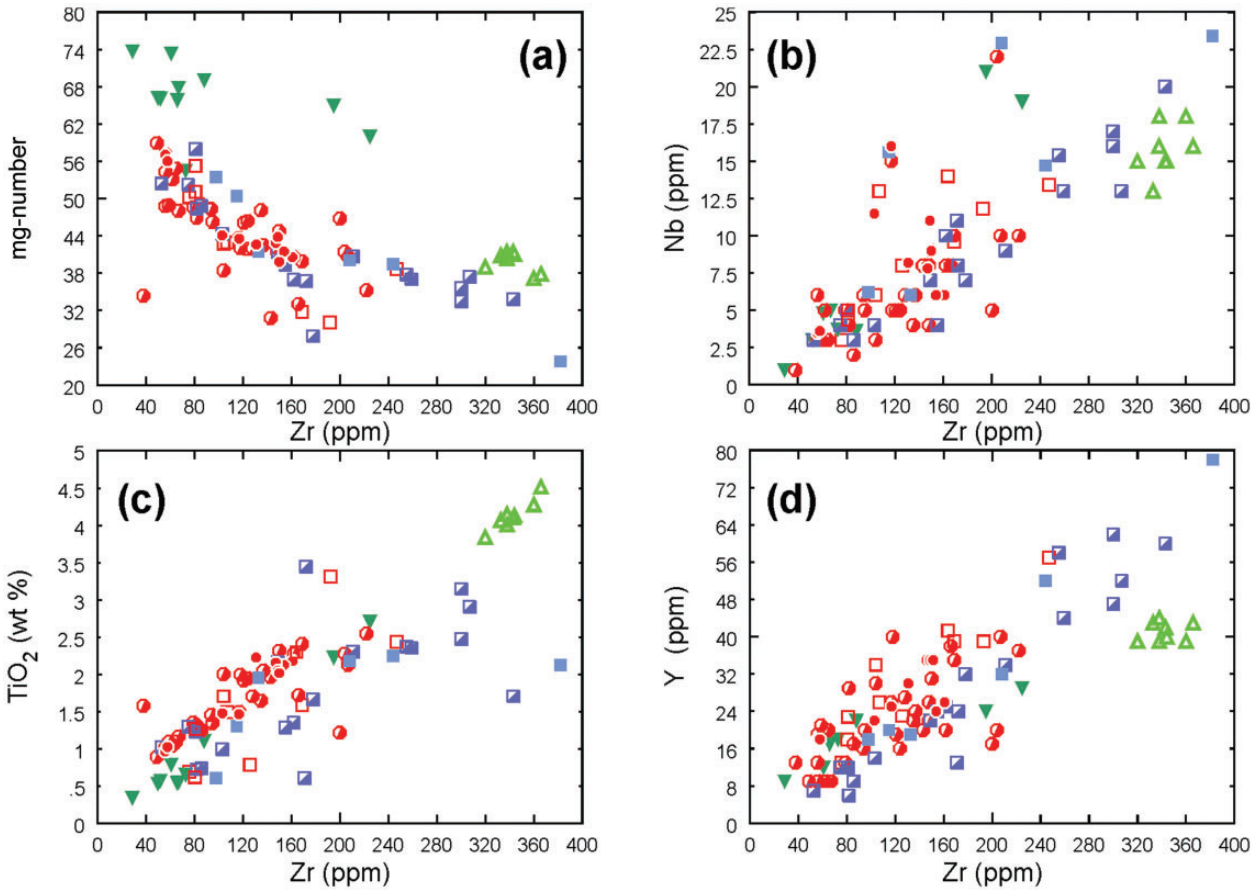

Fig. 13. Selected major and trace elements plots for mafic intrusions from the southern Prince Charles Mountains. Symbols as in Fig. 6.

degree of partial melting results in higher Zr, and also Nb, P, Y, K and REE contents. The flat distribution of the HREE in a low-Zr rock (sPCM29.1) confirms a large degree of partial melting. The elevated LREE abundances in this rock are indicative of derivation from an enriched mantle source region. The rocks with lower concentrations of Zr also contain higher concentrations of SiO_2, Al_2O_3 and CaO, which suggests that clinopyroxene in addition to orthopyroxene and olivine was a constituent of the mantle source. The high CaO/Al_2O_3 ratio is identical to the chondritic CaO/Al_2O_3 (Sun & Nesbitt, 1978) and is consistent with a non-refractory nature for the mantle source. Olivine control can be implied from the good positive correlation between MgO and Ni (Fig. 8e). However, the rocks within the group that have higher Zr and lower SiO_2 contents (lower degrees of partial melting) also have higher Ti/Y and Zr/Y ratios. This implies that Y may have been retained in a restitic phase such as garnet or amphibole, whereas the flat distribution of the heavy REE argues against garnet being present in the restite. A striking feature of this group is the positive correlation between the HFSE abundances and the size of the negative Sr anomaly (Fig. 10a). This may have resulted from either plagioclase fractionation or involvement of plagioclase in progressive partial melting. The more or less constant negative Nb anomalies suggest the magma source was enriched in LREE and LILE, rather than Nb having been retained in a restitic phase. The Sm–Nd isotopic composition also argues for an enriched mantle source. At the same time, the ratio La_N/Yb_N is not high (3·5) and mantle enrichment is thus likely to be only moderate. Alternatively, the La/Nb ratio (1·5–4·4 in all samples) could argue for a considerable role for crustal contamination, but that would cause prominent elevation of Sr_N, which is apparently not the case. Thus a relatively shallow (plagioclase–amphibole-bearing) metasomatically enriched mantle probably served as the source region.

Subalkaline tholeiite

Subalkaline tholeiite dykes include a wide range of compositions suggestive of a complex petrogenesis of more than one coherent magma batch. Dykes of the three spatial suites are similar to each other in terms of major and also some trace elements, which implies that they could share

similar petrogenetic histories. Most of the dykes are highly evolved (generally mg number <50) and crystal fractionation of clinopyroxene and plagioclase may account for most of the systematic trends observed in binary major and major vs trace element diagrams (Figs 7, 8 and 13). This includes, for example, the negative correlation of SiO_2 and MgO, MgO and TiO_2, mg number and Zr, and the positive correlation of MgO and CaO, TiO_2 and Zr. Olivine fractionation is evidenced by positive correlation of MgO and Ni (Fig. 8e), but other element plots (e.g. MgO vs CaO; Fig. 8c) suggest that olivine fractionation was not so important. Strong negative correlations between SiO_2 and TiO_2, and, less evident, between SiO_2 and P_2O_5 imply involvement of magnetite and apatite as fractionating phases. Some rocks are enriched in Fe_2O_3* (up to 20%) and contain skeletal opaque minerals. This does not preclude magnetite fractionation from a similar melt in crustal magma chambers to produce the low-Fe compositions. The lack of phenocryst assemblages—none were found in any of the dyke rocks during this study—may reflect the highly evolved nature of the melts.

A good correlation between incompatible elements (e.g. TiO_2 vs Zr; Fig. 13c) observed for all dyke suites may be explained by either varying degrees of partial melting or crystal fractionation. Fractionation is a more likely process provided that a negative correlation between mg number and incompatible elements (Ti, Zr) is observed. It is worth noting that in some binary plots (e.g. TiO_2 vs MgO, TiO_2 vs Zr, Y vs Zr, Zr vs mg number; Fig. 13) more than one differentiation trend may be observed; these are defined by predominantly either the low-LILE or the high-LILE rocks, reflecting derivation of these groups from somewhat different sources.

The two groups (high-LILE and low-LILE) nevertheless have some similar trace element ratios (Zr/Nb, P/Zr; Table 3), which indicate that they originated from broadly similar mantle source region(s). However, there are many trace element ratios that are different (Ti/Zr, Ti/P, Ti/Y, La/Nb, Ba/Nb, K/Nb, Ce/Y), with the high-LILE group rocks on average showing not only higher LILE/HFSE ratios, but also varying HFSE/HFSE ratios.

Both groups show extensive differentiation trends, and both groups include less fractionated samples (mg number 50–55), although in the high-LILE group such rocks are rare. Extensive within-crust evolution implies that crustal contamination may have modified the magma compositions. However, the low La/Nb ratios (mostly 1–1·5) argue against significant contamination by the local country-rocks. The above-mentioned characteristics of these dykes may be better explained in terms of variable degrees of metasomatic enrichment of their mantle source(s). The less fractionated (higher mg number) high-LILE group rocks show much stronger enrichment in the LILE and LREE, whereas the HFSE are similar to the low-LILE group. Thus it may be suggested that the high-LILE group originated from a much more strongly LILE-enriched mantle source than the low-LILE group rocks, and that the HFSE/HFSE ratios imply considerable differences in the composition of the mantle sources of the two groups. The low-LILE group rocks show only minor to negligible LREE enrichment and their REE distribution patterns are similar to those of enriched mid-ocean ridge (E-MORB)-like basalts. Thus, the bulk composition of the dyke suite may be accounted for by two major mantle source end-members: (1) E-MORB-like pertaining to the NNE suite and the low-LILE group generally; (2) LILE- and LREE-enriched subcontinental mantle, which served as a source for the NW suite and partly for the ENE suite.

Indeed, the high-LILE group rocks have much more enriched compositions in terms of Sm/Nd isotopic ratios with $\varepsilon_{Nd}(0)$ values between −12 and −24 for the NW suite and between −5·5 and −20 for (the high-LILE group) rocks of the ENE suite (Fig. 12). In contrast, the low-LILE group rocks have $\varepsilon_{Nd}(0)$ values between −0·5 and −8 for the NNE-trending suite and −1·5 and −6 for geometrically unassigned rocks of this group ($f^{Sm/Nd}$ mostly between −0·09 and −0·16). These data confirm a suggestion that the two broad geochemical groupings probably reflect different mantle sources, and the consistent younging in T_{DM} model ages would suggest that the low-LILE group rocks were emplaced after the high-LILE group rocks.

There is no strict correspondence of these trends to any particular dyke suite in terms of its strike. However, the NNE-trending dyke rocks have somewhat different trace element ratios (Table 3): K/Rb and Ti/Zr are higher than for the other dyke suites whereas Rb/Sr, Ba/Nb, Th/Nb and Th/U are lower. On the other hand, the NW-trending dykes have lower Ti/Zr, Ti/P and K/Rb, and higher K/Nb, Zr/Nb, Ce/Y and Th/U, indicating derivation from different mantle source(s). Most of the NW-trending dyke rocks have higher Zr, Nb and Y concentrations and lower mg number, pointing to stronger fractionation of these magmas. The ENE suite on the basis of its heterogeneous trace element chemistry may comprise two sub-suites within which the high-LILE group component was potentially older than the low-LILE group.

In terms of the observed dyke suites we would thus conclude that the high-Mg suite is the oldest (notably $T_{DM} > 3$ Ga), followed by three or perhaps four generations of sub-alkaline tholeiites. Of these the NW-trending (± part of ENE-trending suite) are interpreted to be the oldest. These were followed by the rest of ENE-trending dykes, whereas those trending NNE are considered the youngest.

High-Ti–P metabasite

The high-Ti–P metabasite sills are composed of highly evolved (mg number ≤41) rocks with low SiO_2. In most

binary major and trace element plots these rocks form a coherent cluster. In a few plots, for example, SiO_2 vs Fe_2O_3, SiO_2 vs Na_2O (Fig. 7b and d), Zr vs mg number and Zr vs TiO_2 (Fig. 13a and c), linear trends are indicative of crystal fractionation processes. Positive correlation of MgO and Ni indicates olivine control, and other trends such as MgO vs Al_2O_3 and MgO vs CaO (Fig. 8b and c), and negative Sr and Eu anomalies may be accounted for by small degrees of fractionation of clinopyroxene and plagioclase. It is not likely that the overall HFSE and REE enrichment observed in these rocks (Figs 10, 11 and 13) is solely due to crystal fractionation, as this is not confirmed by an inverse relationship between SiO_2 and MgO. It is more likely that the high-Ti–P rocks inherited these geochemical characteristics from their mantle source, and elevated concentrations of most incompatible elements may be due to low degrees of partial melting. Most incompatible trace element ratios have consistent values despite a strong metamorphic overprint, a fact reflected in the linear trends of Zr vs other trace elements (Fig. 13). This implies these rocks are cogenetic and derived from the same or similar mantle sources. However, these rocks have trace element ratios (Table 3) that are distinct from primitive mantle values (Sun & McDonough, 1989): Ti/P and Ti/Zr, for example, have much lower values than primitive mantle, whereas Ce/Y, Zr/Y, Ti/Y and Zr/Nb have higher values. These ratios may reflect a significant role for accessory phases in the mantle source, assuming the partial melting degree was low. The distribution of the REE shows considerable enrichment across the REE spectrum (Fig. 11a). The HREE show nearly flat patterns suggestive of derivation from a garnet-free mantle source. The isotopic Sm–Nd compositions of these rocks indicate their derivation from an enriched (in terms of the LREE) mantle source with $\varepsilon Nd(i) < 0$.

DISCUSSION

High-Mg dykes of early Palaeoproterozoic age are widespread in Enderby Land and the Vestfold Hills. In Enderby Land these intrusions have been dated at 2350 Ma (Sheraton & Black, 1981), whereas in the Vestfold Hills two magmatic pulses are recorded, one at 2425 Ma associated with a comagmatic suite of high-Fe tholeiitic dykes and a second at 2240 Ma (Collerson & Sheraton, 1986; Lanyon *et al.*, 1993). In most major and trace element binary plots the fields of the high-Mg rocks from these two areas nearly completely coincide, although some of the Vestfold Hills rocks have lower SiO_2 contents and the Enderby Land rocks span a wider range for some elements (Fig. 14). The high-Mg rocks from the sPCM are poorly constrained in age; although similar to those from Enderby Land and the Vestfold Hills, they are likely to be the oldest of the observed intrusive suites on the basis of both cross-cutting relationships and T_{DM} model ages (3·1–3·6 Ga). They are constrained to post-date 2820–2780 Ma orogenesis (Boger *et al.*, 2006; Mikhalsky *et al.*, 2010), which is consistent with a single zircon evaporation age of *c.* 2370 Ma reported for this suite (Mikhalsky *et al.*, 1992).

When compared with the Enderby Land and Vestfold Hills dykes (Sheraton & Black 1981; Kuehner, 1989), the high-Mg dykes from the Ruker Complex have basically similar compositions, but tend to contain less SiO_2, Al_2O_3, K_2O and Na_2O, have higher CaO/Al_2O_3, and are more magnesian. With respect to trace elements, many of the incompatible element ratios (e.g. Ti/P, Zr/Nb, Ce/Y) are also basically similar, although important differences are evident (Table 5). For example, the high-Mg dykes from the sPCM generally have higher ratios of Rb/Sr and Ti/Zr. These features may be explained assuming clinopyroxene and plagioclase played an important role during the course of partial melting and subsequent crystal fractionation and precluding a refractory nature of the mantle source. In a mantle-normalized trace element diagram the high-Mg dykes from all three Antarctic areas show a remarkable overlap (Fig. 15a), although the high-Mg dykes from the Ruker Complex are distinguished by lower Th, U, and Pb. These features may at least partly be attributed to the source composition.

In many respects the high-Mg dykes from Enderby Land, the Vestfold Hills, and the sPCM form a continuum of compositions with the Vestfold Hills rocks forming a transitional composition between the sPCM (lower SiO_2, lower K_2O, higher MgO) and the Enderby Land (higher SiO_2, higher K_2O, lower MgO) end-members. On the other hand, Palaeoproterozoic siliceous high-Mg mafic rocks are a common feature of many early Precambrian terranes (Sharkov & Bogina, 2006), and indicate a global mantle evolution feature rather than necessarily indicating a single shared magmatic event.

Dykes of subalkaline tholeiitic composition are also present in all three terranes. Those from the Ruker Complex have chemical characteristics similar to those of typical continental tholeiites in the terms of the ratios of Zr:Ti:Y or Zr:Nb:Y (Fig. 16a and b). In Nb/Yb vs Th/Yb and TiO_2/Yb vs Nb/Yb diagrams (Fig. 16c and d) the subalkaline tholeiites display variable magma–crust interaction and seem to reflect derivation from a slightly enriched (E-MORB-like) mantle source. When compared with tholeiitic dykes in Enderby Land and the Vestfold Hills, the sPCM tholeiites have very similar Ti/P and Zr/Nb ratios, although other trace elements ratios differ (Table 5). Wider similarities emerge when comparing the low-LILE rocks from the sPCM with geochemical Group II of Enderby Land and Group II of the Vestfold Hills. For these rocks nearly identical Ti/Zr, Ce/Y and Rb/Sr ratios are observed (Table 5). However, there are also some noticeable differences; for example, higher K/Rb and K/Nb

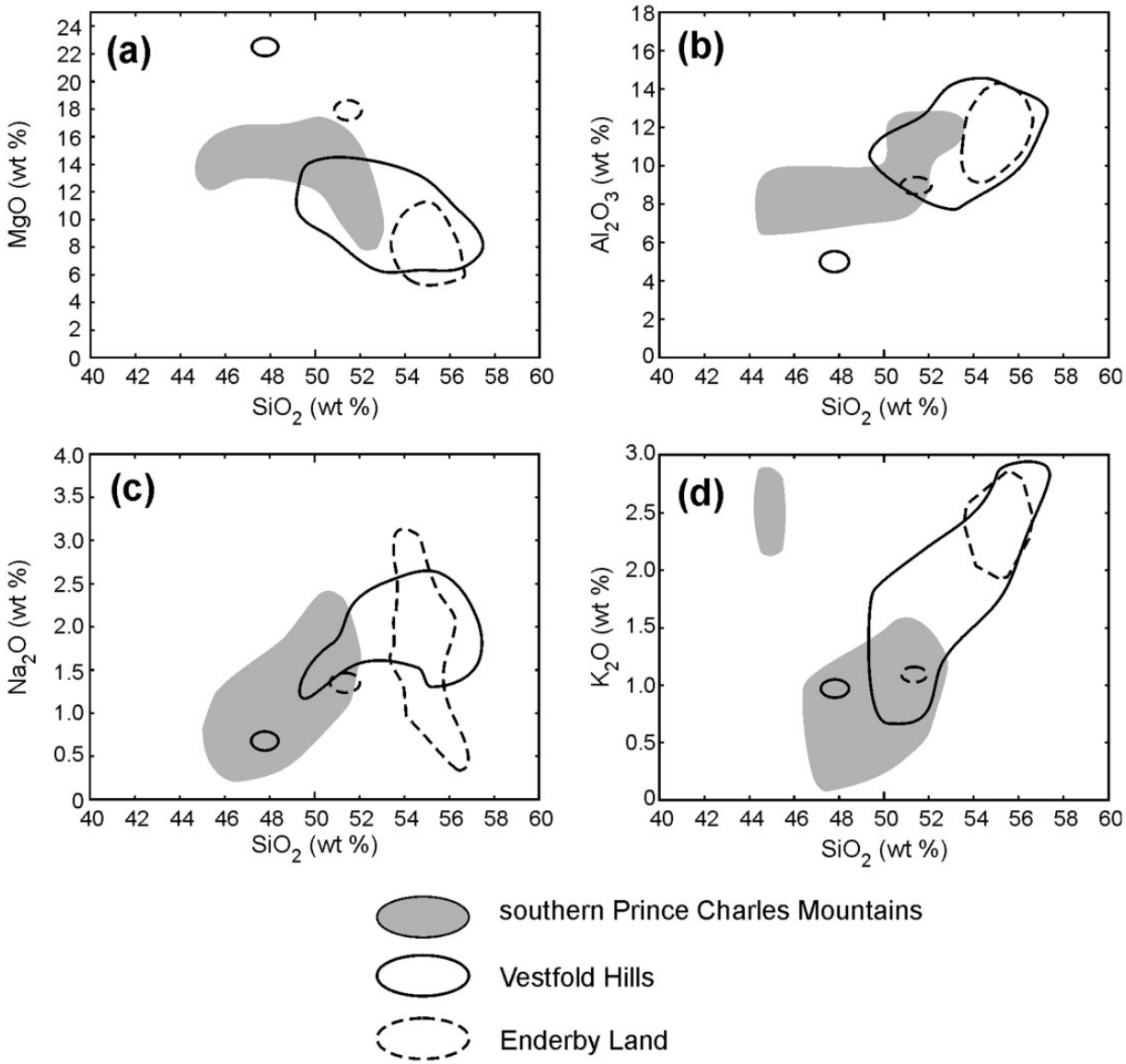

Fig. 14. Fields of high-Mg dyke rocks from the southern Prince Charles Mountains, the Vestfold Hills and the Enderby Land in selected SiO_2–major element oxide plots: (a) MgO; (b) Al_2O_3; (c) Na_2O; (d) K_2O.

ratios are observed for the low-LILE dykes from the sPCM when compared with elsewhere. Kuehner (1986) deduced a primitive mantle source (not having experienced a major melting or enrichment event) for the *c.* 1·38–1·25 Ga dykes in the Vestfold Hills. On the contrary, our data suggest that the roughly coeval dykes in the sPCM were derived from a somewhat enriched mantle source.

Our data also indicate that the Group I rocks from both Enderby Land (*c.* 1·2 Ga) and the Vestfold Hills (*c.* 1·75 Ga) are compositionally most similar to the high-LILE group rocks observed in the Ruker Complex. These broad compositional similarities probably reflect similar mantle processes during the formation of the spatially separated dyke suites, rather than necessarily suggesting a common heritage.

This becomes clear when one considers the numbers and timing of the dyke suites from the different regions. In Enderby Land both Group I (high-LILE) and Group II (low-LILE) tholeiites are comagmatic and belong to either the *c.* 1·2 Ga Ma Amundsen suite (Sheraton & Black, 1981) or the more recently recognized *c.* 2·0–1·9 Ga suite (Suzuki *et al.*, 2008). In the Vestfold Hills three suites of tholeiitic dykes post-date the high-Mg intrusions and these are dated to 1755 Ma, 1380 Ma and 1245 Ma respectively (Black *et al.*, 1991; Lanyon *et al.*, 1993). The 1380 Ma and 1245 Ma suites collectively define the geochemical

Table 5: Selected average incompatible element average ratios for dyke suites from East Antarctic

Ratio	Southern Prince Charles Mountains[1]				Vestfold Hills[2]				Enderby Land[2,3]		
	High-Mg	Low-LILE	High-LILE	High-Ti–P	High-Mg (2·4–2·24 Ga)	Group I (1·75 Ga)	Group II (1·38–1·25 Ga)	Group III (1·38–1·25 Ga)	High-Mg (2·35 Ga)	Group I (1·2 Ga)	Group II (1·2 Ga)
Ti/P	10·65	16·6	10·4	5·5	10·2	7·1	14·1	11·7	9·7	11·2	15·2
K/Rb	250	495	279	320	234	388	314	238	250	308	327
K/Nb	1746	752	1472	330	1842	624	681	461	2011	435	1025
K/Zr	103	37	79	15	87	50	32	35	99	39	35
Ti/Zr	65	95	65	72	57	70	108	82	46	85	97
Zr/Nb	17	21	19	22	20	12	21	13	21	11	29
Ce/Y	1·6	1·0*	1·7†	1·5	1·8	1·7	0·5	0·9	1·8	1·9	0·7
Rb/Sr	0·70	0·06	0·38	0·05	0·39	0·09	0·08	0·19	0·36	0·06	0·10
P/Zr	6·2	6·5	6·4	13·2	6·4	10·2	7·7	7·2	4·8	7·7	6·4
Zr/Y	5·0	4·8	6·0	8·4	4·8	5·4	3·1	3·6	5·4	6·3	3·1
n	10	38	32	8	14	7	20	6	10	19	22

Data sources: [1]this study; [2]J. W. Sheraton (unpublished data); [3]Sheraton & Black (1981).
*$n = 26$.
†$n = 22$.

Groups II and III (Collerson & Sheraton, 1986). It also must be noted that the Vestfold Hills Group I (*c.* 1·75 Ga) rocks represent NW-trending dykes probably derived from an LILE-enriched mantle source (Collerson & Sheraton, 1986; Hoek & Seitz, 1995). A comparison of these rocks with NW-trending dykes (high-LILE group) in the Ruker Complex, however, shows considerable differences in terms of LILE enrichment, especially taking into account the differentiation index mg numbers. Thus, at a given mg number (50–55) NW-trending dykes from the Ruker Complex and the Vestfold Hills contain K_2O 0·3–1·2% and 0·2–0·4%, Rb 15–35 ppm and 4–7 ppm, Ba 100–360 ppm and 50–100 ppm, Sr 165–250 ppm and ~100 ppm, and La 10–20 ppm and 3–4 ppm, respectively. These data indicate that, despite the apparent similarity of the trace element patterns (Fig. 15b), the Vestfold Hills NW-trending dykes were derived from a much less enriched mantle source (Fig. 10g) and/or formed by higher degree of melting than the NW-trending dykes from the Ruker Complex. At the same time, *c.* 1380–1250 Ma Group III tholeiites (Collerson & Sheraton, 1986) demonstrate apparent similarities to the probably Palaeoproterozoic NW-trending suite in the Ruker Complex, rather than with the probably coeval NNE suite intrusions (Fig. 15f).

In the Ruker Complex three to potentially four suites of subalkaline tholeiite post-date the high-Mg suite. The age constraints on these rocks are limited. Each suite post-dates 2·82–2·78 Ga orogenesis observed in the Mawson–Menzies granite–gneiss basement (Boger *et al.*, 2006). This observational constraint, together with the Sm–Nd model ages obtained from these rocks, suggests emplacement ages of <2·78 Ga for the high-LILE component of the ENE suite ($T_{DM} = 2·7–3·8$ Ga) and ≤2·3 Ga for the low-LILE component of the ENE suite ($T_{DM} = 2·3–3·4$ Ga) and the NW suite ($T_{DM} = 2·2–2·9$ Ga). The age of the ENE-trending suite (low-LILE component) is potentially considerably younger than the depleted mantle model ages given the age of *c.* 1350–1300 Ma reported for this suite (Mikhalsky *et al.*, 2007; Fig. 3b). The NNE suite ($T_{DM} = 1·7–2·5$ Ga) is observed to cut the ENE suite, which implies that these rocks must be also <1·3 Ga based on the constraints inferred from the zircon age of Mikhalsky *et al.* (2007).

Elsewhere in the southern Prince Charles Mountains intrusive mafic rocks are mostly absent from the cover sequences to the Mawson–Menzies basement. Mafic intrusions in the form of sills are present within the Sodruzhestvo Group, although these rocks are high-Ti–P and compositionally distinct. Mafic metavolcanic and metamorphosed intrusive rocks of tholeiitic composition are, however, common in the basal sections of the Ruker Group. These rocks have highly variable compositions with Zr/Nb close to chondrite (Mikhalsky *et al.*, 2001). In contrast, consistently higher than chondritic Ba/Zr and K/Zr, albeit with much scatter, suggest melting of LILE-enriched lithospheric mantle and/or involvement of an LILE-rich fluid. Most rocks display marked negative Nb anomalies consistent with the involvement of an LILE-enriched source. The Ruker mafic metavolcanic rocks additionally show smooth REE patterns (Fig. 11e) with only

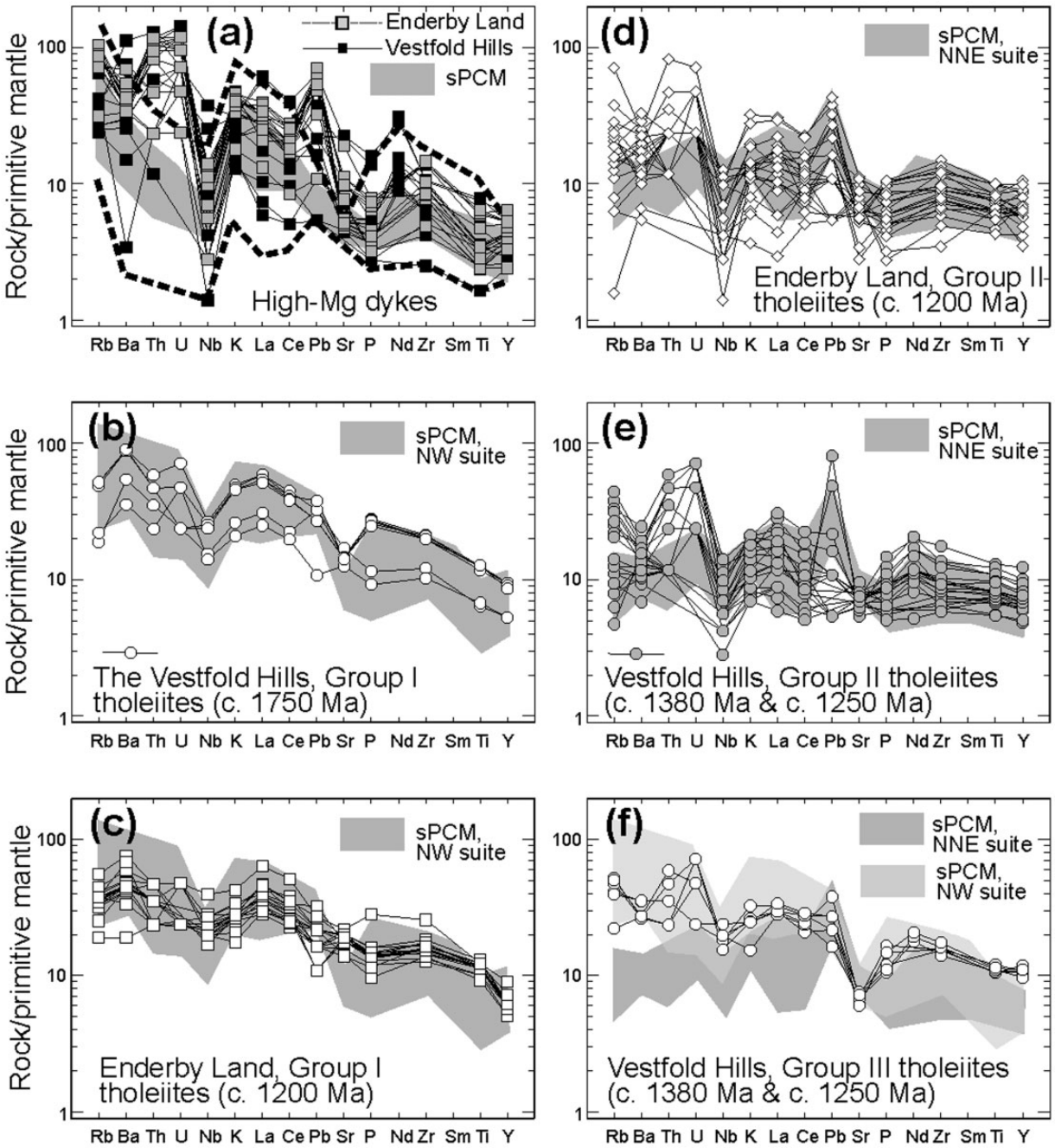

Fig. 15. Primitive mantle normalized trace element patterns for various mafic dyke suites from Enderby Land, the Vestfold Hills with southern Prince Charles Mountains dykes shown for comparison as shaded fields. (a) High-Mg rocks. (b) Group I (*c.* 1750 Ma) high-LILE rocks from the Vestfold Hills. (c) Group I (*c.* 1200 Ma) high-LILE rocks from Enderby Land. (d) Group II (*c.* 1200 Ma) mostly low-LILE rocks from Enderby Land. (e) Group II (*c.* 1380 Ma and *c.* 1250 Ma) mostly low-LILE rocks from the Vestfold Hills. (f) Group III high-LILE rocks from theVestfold Hills. The data for Enderby Land and the Vestfold Hills are largely unpublished data by J. W. Sheraton and also from Sheraton & Black (1981) and Collerson & Sheraton (1986). Normalization factors from Sun & McDonough (1989).

small Eu anomalies and prominent LREE enrichment reflected by $(La/Sm)_N$ between 1·5 and 3·9, whereas $(Sm/Yb)_N$ is between 1·2 and 2·0. Such REE patterns are consistent with partial melting of an enriched mantle source.

Intrusive mafic rocks (dyke metadolerite and sill gabbro–dolerite) from the lowermost Ruker Group show significant compositional similarities to the mafic schists (metavolcanic rocks)—for example, nearly identical or similar Ti/P, Zr/Y, P/Zr, Ti/Zr and some other ratios

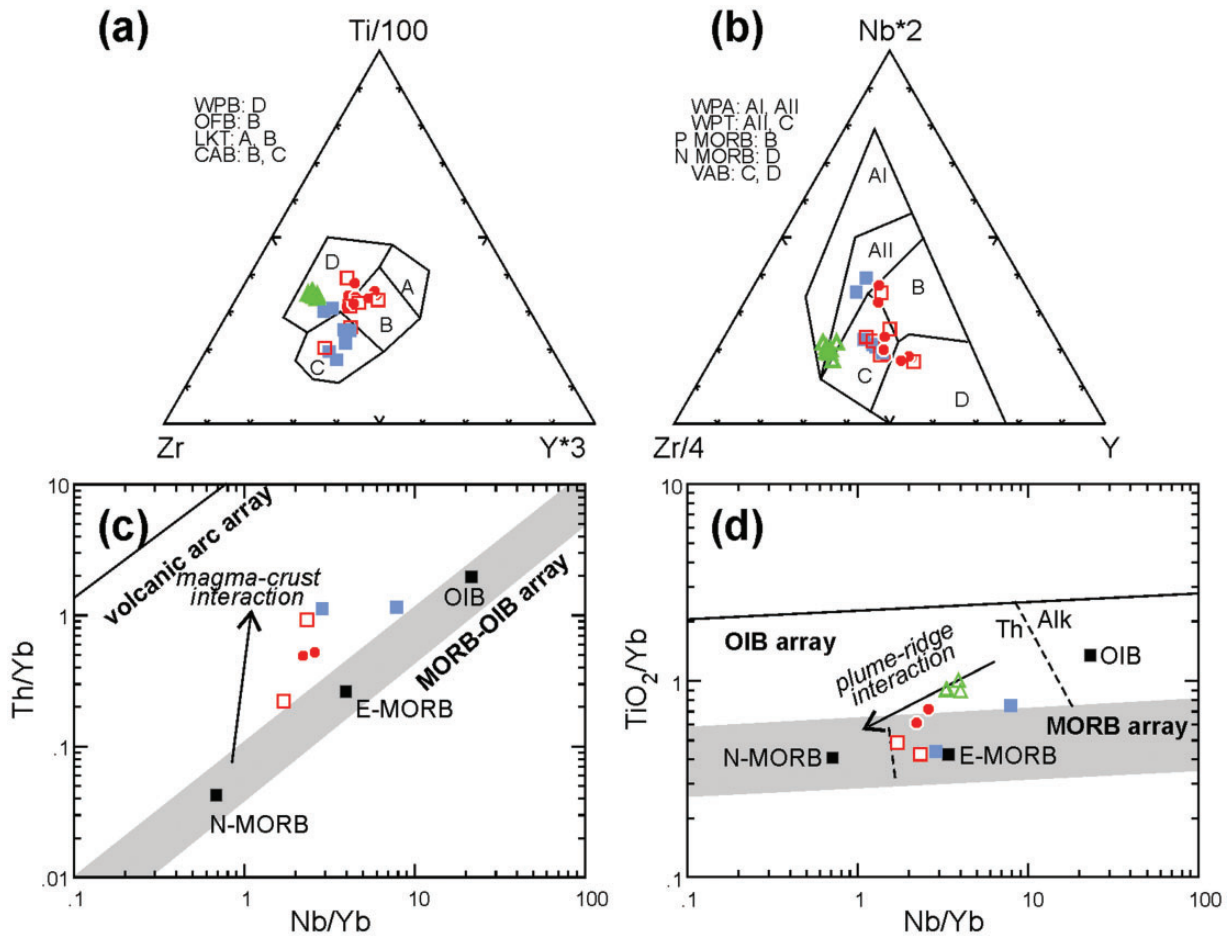

Fig. 16. Trace element discrimination diagrams. (a) Zr–Ti/100–3Y (Pearce & Cann, 1973). (b) Zr/4–2Nb–Y (Meschede, 1986). (c) Nb/Yb vs Th/Yb (Pearce, 2008). (d) Nb/Yb vs TiO_2/Yb (Pearce, 2008). Symbols as in Fig. 6. WPB, within-plate basalts; OFB, ocean floor basalts; LKT, low-K tholeiites; CAB, calc-alkaline basalts; WPA, within-plate alkaline basalts; WPT, within-plate tholeiites; P-MORB, plume-related mid-ocean ridge basalts; E-MORB, enriched mid-ocean ridge basalts; N-MORB, normal mid-ocean ridge basalts; VAB, volcanic arc basalts; OIB, ocean island basalts; Th, tholeiites; Alk, alkaline rocks.

(Table 3)—suggestive of their cogenetic origin (Mikhalsky *et al.*, 2001). Two mafic intrusive rocks from the Ruker Group also yield Sm–Nd T_{DM} ages of *c.* 2·9–3·0 Ga and $\varepsilon_{Nd}(0)$ of −17 to −18 (E. V. Mikhalsky, unpublished data).

Considering the dyke groups adopted in this study, some striking similarities exist between the Ruker Group mafic rocks and the NW-trending suite observed in the Mawson Escarpment. The Ruker metavolcanic and intrusive rocks (especially dykes) and the NW dyke suite are all high-LILE bearing rocks and have similar Zr/Y, Ti/Zr, La/Nb, Zr/Nb and Ti/Y ratios (Table 3), albeit the NW-trending dykes are more strongly fractionated (mg number 24–55, compared with 35–60 in the Ruker Group rocks; Mikhalsky *et al.*, 2001). Other trace element ratios are somewhat different (K/Nb, Ce/Y and K/Zr), although the NW-trending dykes (Fig. 10c) and mafic rocks from Ruker Group (Fig. 10f) nevertheless display very similar trace element patterns. The Nd isotope compositions of both the mafic intrusive rocks at Mt Ruker and the NW dyke suite also overlap. For the Mt Ruker metagabbro–dolerites T_{DM} ages are 2·9–3·0 Ga and $\varepsilon_{Nd}(0)$ of −17 to −18, compared with 2·3–2·9 Ga and −12 to −24 for the NW dyke suite. NW- to WNW-trending mafic dykes are also present in a Mawson suite granitic pluton exposed in the NE of Mt Ruker and these, albeit from a limited dataset (E. V. Mikhalsky, unpublished data), appear to resemble the NW dyke suite. Assuming the high-LILE characteristics and similar Nd isotopic systematics observed for the NW dyke suite and the lowermost Ruker Group mafic rocks do reflect a cogenetic origin, we suggest that the data obtained for these rocks imply that the Ruker Group was deposited after 2·3 Ga, somewhat younger that the maximum depositional ages obtained for detrital zircons from these rocks (Phillips *et al.*, 2006).

It should be noted that secular mantle evolution from a reservoir that is more enriched in highly incompatible

elements in the Palaeoproterozoic to one that is less enriched or primitive has been proposed by Sheraton & Black (1981), Collerson & Sheraton (1986), Hoek & Seitz (1995) and Suzuki *et al.* (2008), based on petrological studies in Enderby Land and the Vestfold Hills. Those researchers basically argued for a largely convergent plate boundary setting or a gravitationally unstable crustal regime in these areas during the Palaeoproterozoic and for upwelling asthenosphere (as a linear sheet) during the mid-Mesoproterozoic. The asthenospheric component is best exemplified by the alkaline dykes: alkali basalts in Enderby Land (Suzuki *et al.*, 2008) and calc-alkaline to ultramafic lamprophyres in the Vestfold Hills (Mikhalsky *et al.*, 1992). Our investigation failed to discover any Precambrian mafic alkaline dykes in the sPCM, which may be due to insufficient lithosphere thickness and rigidity. Otherwise our data are in accord with the proposed secular mantle evolution, which is reflected in decreasing LILE/HFSE ratios (e.g. K/Zr, Ce/Y, Tables 3 and 5).

At Cumpston Massif low-grade metasediments of the Sodruzhestvo Group contain mafic sills and dykes that were earlier attributed to the same presumed mid-Mesoproterozoic intrusive event that led to the emplacement of the dyke suites in the Mawson–Menzies basement rocks (Tingey, 1982). These rocks, however, have distinct high-Ti–P compositions and thus do not correlate with the other dyke groups observed elsewhere in the sPCM, or for that matter with the dyke suites observed in other areas of East Antarctica. A mafic sill in Mt Seddon, where the Sodruzhestvo Group also crops out, has an identical high-Ti–P composition (Table 1). In tectonic discrimination diagrams (Fig. 16), these rocks compositionally correspond to within-plate magmas probably derived from an ocean island basalt-type source. Mafic sills and dykes at Cumpston Massif are thus interpreted to be plume related and probably originated during an advanced stage of extension in the course of formation of the Sodruzhestvo basin.

CONCLUSIONS

(1) High-Mg rocks from the Ruker Complex have T_{DM} model ages of 3·6–3·1 Ga and are constrained on geological grounds to have been emplaced sometime after 2780 Ma. These rocks are in general strongly recrystallized and sheared. Pseudomorphs indicate orthopyroxene as a primary magmatic phase. These rocks were probably derived by varying degrees of partial melting of a metasomatically enriched and radiogenic mantle source at relatively shallow mantle levels. These rocks have many features in common with the early Palaeoproterozoic (2·40–2·25 Ga) high-Mg dykes from Enderby Land and the Vestfold Hills, although they remain chemically distinct (lower SiO_2, lower K_2O, higher MgO) and cannot be directly correlated.

(2) Abundant subalkaline tholeiitic mafic dykes in the Mawson Escarpment strike generally NNE, NW or ENE. Two geochemically distinct rock groups may be distinguished: a low-LILE group and a high-LILE group. In terms of age, the sequence of emplacement is taken to be NW, ENE, then NNE.

(2a) The high-LILE group rocks are represented by the NW-trending dykes and a component of the ENE suite. These rocks are characterized by higher LILE/HFSE ratios, implying that they were derived from an REE-enriched but inhomogeneous subcontinental mantle source. The model ages for these rocks are mostly older than those obtained from the low-LILE group rocks. For the NW-trending suite T_{DM} model ages are 2·30–2·90 Ga, whereas for the ENE-trending dykes of this composition T_{DM} model ages are 2·70–3·85 Ga.

(2b) The low-LILE group rocks include all the NNE-trending suite of dykes as well as a component of the ENE-trending suite. These rocks probably originated from an E-MORB-like mantle source region. The model ages for these rocks are mostly between 1·7 and 2·5 Ga for the NNE suite and 2·3 and 3·4 Ga for the ENE suite. The low-LILE component of the ENE suite is inferred to have been emplaced in the Mesoproterozoic (*c.* 1350–1300 Ma; Mikhalsky *et al.*, 2007), which, on the basis of field constraints, suggests that the NNE-trending suite was emplaced somewhat after this time.

(3) Similarities between the NW-trending subalkaline tholeiitic dykes and the extrusive volcanic or subvolcanic rocks in the Palaeoproterozoic Ruker Group suggest a common or very similar LILE-enriched mantle source. This points to a possible cogenetic and roughly coeval origin for these rocks. Thus the dykes may represent within-basement counterparts of the volcanic fill of the Mt Ruker aulocogene.

(4) Our data confirm observations made by Sheraton & Black (1981) and Collerson & Sheraton (1986) on secular mantle evolution between the Palaeoproterozoic and late Mesoproterozoic. Those workers concluded that the Palaeoproterozoic dyke sources in both Enderby Land and Vestfold Hills were more enriched in highly incompatible elements than those of the younger tholeiites.

(5) High-Ti–P mafic sills and minor dykes occur within the Sodruzhestvo Group exposed at Cumpston Massif and Mt Seddon. These rocks have very distinctive transitional to alkaline compositions and may not be correlated with any other dyke suite in the sPCM or elsewhere in East Antarctica (to the authors' knowledge). These rocks are within-plate

plume-related magmatic manifestations of Neoproterozoic extension, crustal subsidence and sediment accumulation, probably reflecting the break-up of the Rodinia supercontinent.

(6) As observed by earlier researchers, the subalkaline tholeiitic dykes in the Ruker Complex have many compositional features in common with mafic dykes from the Napier Complex of Enderby Land and from the Vestfold Hills. Most striking similarities are found between the low-LILE group rocks (NNE and partly ENE suites) from the Ruker Complex and the *c.* 1250 Ma dykes (Group II rocks) from the Vestfold Hills. Nevertheless, notable compositional differences exist between the mafic intrusive rocks from these three regions. For example, the high-LILE group rocks from the sPCM (NW suite) differ considerably from the Group I (high-LILE) dykes in the Vestfold Hills (*c.* 1750 Ma). Similarly, some of the alkaline and compositionally intermediate rocks observed in the Napier Complex (Suzuki *et al.*, 2008) have no direct comparatives in the Ruker Complex; similarly, there are no direct correlatives for the high-Ti–P rocks observed within the Sodruzhestvo Group within either the Napier Complex or the Vestfold Hills. These features do not provide convincing evidence for a direct correlation of dyke suites in the Ruker Complex, Enderby Land, and the Vestfold Hills. It is thus more likely that these terranes did not experience a common geological history, at least not before the mid-Mesoproterozoic (Mikhalsky & Sheraton, 2011) but arguably not before the Cambrian (Boger *et al.*, 2001; Boger, 2011). This is consistent with recently published feldspar Pb-isotope data that highlight the strikingly different Pb compositions of the Napier and Vestfold complexes when compared with the Ruker Complex (Flowerdew *et al.*, 2013). Whereas the coastal Napier and Vestfold complexes have Pb isotopic compositions that plot well above the Pb isotope growth curve and correlate with parts of cratonic India, the Pb isotopic compositions of the Ruker Complex are unradiogenic and, consistent with the different magmatic history described here, imply these rocks were derived from different protoliths that have protracted, but unrelated, histories.

ACKNOWLEDGEMENTS

The geological data were mostly collected during the PCMEGA 2002–2003 expedition, with logistic support by the Australian Antarctic Division. R. Maas (The University of Melbourne) is greatly thanked for his skill and expertise in carrying out the Sm–Nd analyses and help with a summary of analytical procedures. Dr J. W. Sheraton is greatly thanked for providing the geochemical database on the mafic dykes from the southern Prince Charles Mountains, the Enderby Land, and the Vestfold Hills. The manuscript benefited from thorough and helpful reviews by J. Halpin and two anonymous reviewers.

FUNDING

The work was partly supported by Deutsche Forschungsgemeinschaft (DFG) grant RO 3038/1-1 and Russian Foundation for Basic Research (RFBR) grant 11-05-00254 to E.V.M.

SUPPLEMENTARY DATA

Supplementary data for this paper are available at *Journal of Petrology* online.

REFERENCES

Black, L. P. & James, P. R. (1983). Geological history of the Napier Complex of Enderby Land. In: Oliver, R. L., James, P. R. & Jago, J. B. (eds) *Antarctic Earth Science*. Australian Academy of Science, pp. 11–15.

Black, L. P., Kinny, P. D. & Sheraton, J. W. (1991). The difficulties of dating mafic dykes: an Antarctic example. *Contributions to Mineralogy and Petrology* **109**, 183–194.

Boger, S. D. (2011). Antarctica—before and after Gondwana. *Gondwana Research* **19**, 335–371.

Boger, S. D. & Wilson, C. J. L. (2005). Early Cambrian crustal shortening and a clockwise *P–T–t* path from the southern Prince Charles Mountains, East Antarctica: implications for the formation of Gondwana. *Journal of Metamorphic Geology* **23**, 603–623.

Boger, S. D., Wilson, C. J. L. & Fanning, C. M. (2001). Early Paleozoic tectonism within the East Antarctic Craton: the final suture between east and west Gondwana? *Geology* **29**, 463–466.

Boger, S. D., Wilson, C. J. L. & Fanning, C. M. (2006). An Archaean province in the southern Prince Charles Mountains, East Antarctica: U–Pb zircon evidence for *c.* 3170 Ma granite plutonism and *c.* 2780 Ma partial melting and orogenesis. *Precambrian Research* **145**, 207–228.

Boger, S. D., Maas, R. & Fanning, C. M. (2008). Isotopic and geochemical constraints on the age and origin of granitoids from the central Mawson Escarpment, southern Prince Charles Mountains, East Antarctica. *Contributions to Mineralogy and Petrology* **155**, 379–400.

Collerson, K. D. & Sheraton, J. W. (1986). Age and geochemical characteristics of a mafic dyke swarm in the Archaean Vestfold Block, Antarctica: inferences about Proterozoic dyke emplacement in Gondwana. *Journal of Petrology* **27**, 853–886.

Condie, K. (1989). *Plate Tectonics and Crustal Evolution*. Pergamon, 288 p.

Corvino, A. F. & Henjes-Kunst, F. (2007). A record of 2·5 and 1·1 billion year old crust in the Lawrence Hills, Antarctic Southern Prince Charles Mountains. *Terra Antartica* **14**, 13–30.

Corvino, A. F., Boger, S. D., Henjes-Kunst, F., Wilson, C. J. L. & Fitzsimons, I. C. W. (2008). Superimposed tectonic events at 2450 Ma, 2100 Ma, 900 Ma and 500 Ma in the North Mawson Escarpment, Antarctic Prince Charles Mountains. *Precambrian Research* **167**, 281–302.

Corvino, A. F., Wilson, C. J. L. & Boger, S. D. (2011). The structural and tectonic evolution of a Rodinian continental fragment in the Mawson Escarpment, Prince Charles Mountains, Antarctica. *Precambrian Research* **184**, 70–92.

Crohn, P. W. (1959). *A contribution to the geology and glaciology of the western part of Australian Antarctic Territory. Bureau of Mineral Resources Australia Bulletin* **52**.

Crawford, A. J., Falloon, T. J. & Green, D. H. (1989). Classification, petrogenesis and tectonic setting of boninites. In: Crawford, A. J. (ed.) *Boninites and Related Rocks*. Unwin Hyman, pp. 1–49.

DePaolo, D. J. (1988). *Neodymium Isotope Geochemistry: an Introduction*. Springer, 187 p.

England, R. N. & Langworthy, A. P. (1975). *Geological work in Antarctica—1974. Bureau of Mineral Resources Australia Record* **1975/30**.

Fedorov, L. V., Grikurov, G. E., Kurinin, R. G. & Masolov, V. N. (1982). Crustal structure of the Lambert Glacier area from geophysical data. In: Craddock, C. (ed.) *Antarctic Geoscience*. University of Wisconsin Press, pp. 931–936.

Flowerdew, M. J., Tyrrell, S., Boger, S. D., Fitzsimons, I. C. W., Harley, S. L., Mikhalsky, E. V. & Vaughan, A. P. M. (2013). Pb isotopic domains from the Indian Ocean sector of Antarctica: implications for past Antarctica–India connections. In: Harley, S. L., Fitzsimons, I. C. W. & Zhao, Y. (eds) *Antarctica and Supercontinent Evolution. Geological Society, London, Special Publications*, V. 383, http://dx.doi.org/10.1144/SP1383.1143.

Goldstein, S. J. & Jacobsen, S. B. (1988). Nd and Sr isotopic systematics of river water suspended material: implications for crustal evolution. *Earth and Planetary Science Letters* **87**, 249–265.

Grew, E. S. (1982). Geology of the southern Prince Charles Mountains, east Antarctica. In: Craddock, C. (ed.) *Antarctic Geoscience*. University of Wisconsin Press, pp. 473–478.

Grikurov, G. E. & Soloviev, D. S. (1974). Geologicheskoe stroenie gornogo obramlenia lednika Lamberta. *Soviet Antarctic Expedition Bulletin* **88**, 21–29.

Halpin, J. A., Gerakiteys, C., Clarke, G. L., Belousova, E. A. & Griffin, W. L. (2005). *In-situ* U–Pb geochronology and Hf isotope analyses of the Rayner Complex, east Antarctica. *Contributions to Mineralogy and Petrology* **148**, 689–706.

Hoek, J. D. & Seitz, H.-M. (1995). Continental mafic dyke swarms as tectonic indicators: an example from the Vestfold Hills, East Antarctica. *Precambrian Research* **75**, 121–139.

Iltchenko, L. N. (1972). Late Precambrian acritarchs of Antarctica. In: Adie, R. J. (ed.) *Antarctic Geology and Geophysics*. Universitetsforlaget, pp. 599–602.

Jacobsen, S. B. & Wasserburg, G. J. (1984). Sm–Nd evolution of chondrites and achondrites. II. *Earth and Planetary Science Letters* **67**, 137–150.

Kamenev, E. N. (1982). Regional metamorphism in Antarctica. In: Craddock, C. (ed.) *Antarctic Geoscience*. University of Wisconsin Press, pp. 429–433.

Kamenev, E. N., Andronikov, A. V., Mikhalsky, E. V., Krasnikov, N. N. & Stüwe, K. (1993). Soviet geological maps of the Prince Charles Mountains. *Australian Journal of Earth Sciences* **40**, 501–517.

Kelly, N. M., Clarke, G. L. & Fanning, C. M. (2004). Archaean crust in the Rayner Complex of east Antarctica: Oygarden Group of islands, Kemp Land. *Transactions of the Royal Society of Edinburgh: Earth Sciences* **95**, 491–510.

Kuehner, S. M. (1986). Mafic dykes of the East Antarctic shield: experimental, geochemical and petrological studies focusing on the Proterozoic evolution of the crust and mantle, PhD thesis, University of Tasmania, Hobart.

Kuehner, S. M. (1987). Mafic dykes of the East Antarctic shield: a note on the Vestfold Hills and Mawson Coast occurrences in mafic dyke swarms. In: Halls, H. C. & Fahrig, W. F. (eds) *Mafic Dyke Swarms. Geological Association of Canada, Special Papers* **34**, 4219–430.

Kuehner, S. M. (1989). Petrology and geochemistry of early Proterozoic high-Mg dykes from the Vestfold Hills, Antarctica. In: Crawford, A. J. (ed.) *Boninites and Related Rocks*. Unwin Hyman, pp. 208–231.

Lanyon, R., Black, L. P. & Seitz, H-M. (1993). U–Pb zircon dating of mafic dykes and its application to the Proterozoic geological history of the Vestfold Hills, East Antarctica. *Contributions to Mineralogy and Petrology* **115**, 184–203.

Le Maitre, R. W. (1989). *A Classification of Igneous Rocks and Glossary of Terms*. Blackwell Scientific.

Lopatin, B. G. & Semenov, V. S. (1982). Amphibolite facies rocks of the southern Prince Charles Mountains, East Antarctica. In: Craddock, C. (ed.) *Antarctic Geoscience*. University of Wisconsin Press, pp. 465–471.

Maas, R., Kamenetsky, M. B., Sobolev, A. V., Kamenetsky, V. S. & Sobolev, N. V. (2005). Sr–Nd–Pb isotopic evidence for a mantle origin of alkali chlorides and carbonates in the Udachnaya kimberlite, Siberia. *Geology* **35**, 549–552.

Meschede, M. (1986). A method of discriminating between different types of mid-ocean ridge basalts and continental tholeiites with the Nb–Zr–Y diagram. *Chemical Geology* **56**, 207–218.

McLean, M., Rawling, T. J., Betts, P. G., Phillips, G. & Wilson, C. J. L. (2008). Three-dimensional inversion modelling of a Neoproterozoic basin in the southern Prince Charles Mountains, East Antarctica. *Tectonophysics* **456**, 180–193.

McLeod, I. R. (1959). *Report on the geological and glaciological work by the 1958 Australian National Research Expedition. Bureau of Mineral Resources Australia Record* **1959/131**.

McLeod, I. R. (1964). An outline of the geology of the sector longitude 45°E to 80°E, Antarctica. In: Adie, R. J. (ed.) *Antarctic Geology*. New Holland, pp. 237–247.

Mikhalsky, E. V. (1995). Proterozoic mafic dykes in Vestfold Oasis, East Antarctica. *Antarctica, Commission Reports* **33**, 19–36 (in Russian).

Mikhalsky, E. V. & Sheraton, J. W. (2011). The Rayner tectonic province of East Antarctica: compositional features and geodynamic setting. *Geotectonics* **45**, 496–512.

Mikhalsky, E. V., Andronikov, A. V. & Beliatsky, B. V. (1992). Mafic igneous suites in the Lambert rift zone. In: Yoshida, Y., Kaminuma, K. & Shiraishi, K. (eds) *Recent Progress in Antarctic Earth Sciences*. Terra, pp. 173–178.

Mikhalsky, E. V., Andronikov, A. V., Beliatsky, B. V. & Kamenev, E. N. (1993). Mafic and ultramafic igneous suites in the Lambert–Amery rift zone. In: Findlay, R. H., Unrug, R., Banks, M. R. & Veevers, J. J. (eds) *Gondwana Eight*. A. A. Balkema, pp. 541–546.

Mikhalsky, E. V., Sheraton, J. W., Laiba, A. A., Tingey, R. J., Thost, D. E., Kamenev, E. N. & Fedorov, L.V. (2001). *Geology of the Prince Charles Mountains, Antarctica. AGSO–Geoscience Australia Bulletin* **247**, 209 p.

Mikhalsky, E. V., Beliatsky, B. V., Sheraton, J. W. & Roland, N.W. (2006*a*). Two distinct Precambrian terranes in the southern Prince Charles Mountains, East Antarctica: SHRIMP dating and geochemical constraints. *Gondwana Research* **9**, 291–309.

Mikhalsky, E. V., Laiba, A. A. & Beliatsky, B. V. (2006*b*). The composition of the Prince Charles Mountains: a review of geologic and isotopic data. In: Fütterer, D. K., Damaske, D., Kleinschmidt, G., Miller, H. & Tessensohn, F. (eds) *Antarctica: Contributions to Global Earth Sciences*. Springer, pp. 69–82.

Mikhalsky, E. V., Henjes-Kunst, F., Belyatsky, B. V. & Roland, N. W. (2007). Mafic dykes in the southern Prince Charles Mountains: A tale of Pan-African amalgamation of East Antarctica questioned. In: Cooper, A. K. & Raymond, C. R. *et al.* (eds) *Antarctica: A Keystone in a Changing World. Online Proceedings of the 10th ISAES. US Geological Survey Open-File Report* **2007-1047**, Extended Abstract 014, 4 pp.

Mikhalsky, E. V., Belyatsky, B. V. & Roland, N. W. (2008). New evidence for Palaeoproterozoic tectono-magmatic activities in the southern Prince Charles Mountains, East Antarctica. *Polarforschung* **78**, 85–94.

Mikhalsky, E. V., Henjes-Kunst, F., Belyatsky, B. V., Roland, N. W. & Sergeev, S. A. (2010). New Sm–Nd, Rb–Sr, U–Pb and Hf isotope systematics for the southern Prince Charles Mountains (East Antarctica) and its tectonic implications. *Precambrian Research* **182**, 101–123.

Pearce, J. A. (2008). Geochemical fingerprinting of oceanic basalts with applications to ophiolite classification and the search for Archean oceanic crust. *Lithos* **100**, 14–48.

Pearce, J. A. & Cann, J. R. (1973). Tectonic setting of basic volcanic rocks determined using trace element analysis. *Earth and Planetary Science Letters* **19**, 290–300.

Phillips, G., Wilson, C. J. L. & Fitzsimons, I. C. W. (2005). Stratigraphy and structure of the southern Prince Charles Mountains, East Antarctica. *Terra Antartica* **12**, 69–86.

Phillips, G., Wilson, C. J. L., Campbell, I. H. & Allen, C. M. (2006). U–Th–Pb detrital zircon geochronology from the southern Prince Charles Mountains, East Antarctica—defining the Archaean to Neoproterozoic Ruker province. *Precambrian Research* **148**, 292–306.

Phillips, G., Wilson, C. J. L., Phillips, D. & Szcepanski, S. K. (2007). Thermochronological ($^{40}Ar/^{39}Ar$) evidence of Early Palaeozoic basin inversion within the southern Prince Charles Mountains, East Antarctica: implications for East Gondwana. *Journal of the Geological Society, London* **164**, 771–784.

Phillips, G., Kelsey, D. E., Corvino, A. F. & Dutch, R. A. (2009). Continental reworking during overprinting orogenic events, southern Prince Charles Mountains, East Antarctica. *Journal of Petrology* **50**, 2017–2041.

Raczek, I., Stoll, B., Hofmann, A.W. & Jochum, K. P. (2000). High-precision trace element data for the USGS reference materials BCR-1, BCR-2, BHVO-1, BHVO-2, AGC-1, AGV-2, DTS-1, DTS-2, GSP-1 and GSP-2 by ID-TIMS and MIC-SSMS. *Geostandards Newsletter* **25**, 77–86.

Raczek, I., Jochum, K. P. & Hofmann, A. W. (2003). Neodymium and strontium isotope data for USGS reference materials BCR-1, BCR-2, BHVO-1, BHVO-2, AGV-1, AGV-2, GSP-1, GSP-2 and eight MPI-DING reference glasses. *Geostandards Newsletter* **27**, 173–179.

Ravich, M. G. (1982). The lower Precambrian of Antarctica. In: Craddock, C. (ed.) *Antarctic Geoscience*. University of Wisconsin Press, pp. 421–428.

Ravich, M. G. & Fedorov, L. V. (1982). Geologic structure of MacRobertson Land and Prince Elizabeth Land, East Antarctica. In: Craddock, C. (ed.) *Antarctic Geoscience*. University of Wisconsin Press, pp. 499–504.

Ravich, M. G., Soloviev, D. S. & Federov, L. V. (1985). *Geological Structure of MacRobertson Land (East Antarctica)*. A. A. Balkema.

Ruker, R. A. (1963). *Geological reconnaissance in Enderby Land and the southern Prince Charles Mountains. Bureau of Mineral Resources Australia Record* **1963/154**.

Sharkov, E. V. & Bogina, M. M. (2006). Evolution of Paleoproterozoic magmatism: geology, geochemistry, and isotopic constraints. *Stratigraphy and Geological Correlation* **14**, 345–367.

Sheraton, J. W. & Black, L. P. (1981). Geochemistry and geochronology of Proterozoic tholeiite dykes of East Antarctica: evidence for mantle metasomatism. *Contributions to Mineralogy and Petrology* **78**, 305–317.

Sheraton, J. W. & Labonne, B. (1978). *Petrology and geochemistry of acid igneous rocks of northeast Queensland. Bureau Mineral Resources Australia Bulletin* **169**.

Sheraton, J. W., Thomson, J. W. & Collerson, K. D. (1987). Mafic dyke swarms of Antarctica. In: Halls, H. C. & Fahrig, W. F. (eds) *Mafic Dyke Swarms. Geological Association of Canada, Special Papers* **34**, 419–432.

Soloviev, D. S. (1972). Geological structure of the mountain fringe of the Lambert Glacier and Amery Ice Shelf. In: Adie, R. J. (ed.) *Antarctic Geology and Geophysics*. Universitetsforlaget, pp. 573–577.

Srivastava, R. K., Singh, R. K. & Verma, R. (2000). Juxtaposition of India and Antarctica during the Precambrian: inferences from geochemistry of mafic dykes. *Gondwana Research* **3**, 227–234.

Stinear, B. H. (1956). *Preliminary report on operations from Mawson base, Australian National Antarctic Research Expedition 1954–55. Bureau of Mineral Resources Australia Record* **1956/44**.

Sun, S-S. & McDonough, W. F. (1989). Chemical and isotopic systematics of oceanic basalts: implications for mantle composition and processes. In: Saunders, A. D. & Norry, M. J. (eds) *Magmatism in the Ocean Basins. Geological Society, London, Special Publications* **42**, 313–345.

Sun, S.-S. & Nesbitt, R. W. (1978). Geochemical regularities and genetic significance of ophiolitic basalts. *Geology* **6**, 689–693.

Suzuki, S., Ishizuka, H. & Kagami, H. (2008). Early to middle Proterozoic dykes in the Mt. Riiser–Larsen area of the Napier Complex, East Antarctica: tectonic implications as deduced from geochemical studies. In: Satish-Kumar, M., Motoyoshi, Y., Osanai, Y., Hiroi, Y. & Shiraishi, K. (eds) *Geodynamic Evolution of East Antarctica: a Key to the East–West Gondwana Connection. Geological Society, London, Special Publications* **308**, 195–210.

Tingey, R. J. (1982). The geologic evolution of the Prince Charles Mountains—an Antarctic Archean cratonic block. In: Craddock, C. (ed.) *Antarctic Geoscience*. University of Wisconsin Press, pp. 455–464.

Tingey, R. J. (1991). The regional geology of Archaean and Proterozoic rocks in Antarctica. In: Tingey, R. J. (ed.) *The Geology of Antarctica*. Clarendon Press, pp. 1–58.

Tingey, R. J. & England, R. N. (1973). *Geological work in Antarctica—1972. Bureau of Mineral Resources Australia Record* **1973/161**.

Tingey, R. J., England, R. N. & Sheraton, J. W. (1981). *Geological investigations in Antarctica 1973—The southern Prince Charles Mountains. Bureau of Mineral Resources Australia Record* **1981/43**.

Trail, D. S. (1963*a*). Low-grade metamorphic rocks from the Prince Charles Mountains, East Antarctica. *Nature* **197**, 548–550.

Trail, D. S. (1963*b*). *The 1961 geological reconnaissance in the southern Prince Charles Mountains. Bureau of Mineral Resources Australia Record* **1963/155**.

Trail, D. S. (1964). Schist and granite in the southern Prince Charles Mountains. In: Adie, R. J. (ed.) *Antarctic Geology*. New Holland, pp. 492–497.

Weis, D., Kieffer, B., Maerschalk, C., Barling, J., Jong, J. D., Williams, G. A., Hanano, D., Pretorius, W., Mattielli, M., Scoates, J. S., Goolaerts, A., Friedman, R. M. & Mahoney, J. B. (2006). High-precision isotopic characterization of USGS reference materials by TIMS and MC-ICP-MS. *Geochemistry, Geophysics, Geosystems* **7(8)**, doi:10.1029/2006GC001283.